Forward charm production and intrinsic charm in the nucleon: constraints from the IceCube Neutrino Observatory and sinergy with the LHC forward experiments

Rafał Maciuła

Institute of Nuclear Physics PAN, Kraków, Poland

in collaboration with A. Szczurek, V.P. Goncalves
based on: arXiv:2103.05503 [hep-ph], arXiv:2105.09370 [hep-ph]
and Phys. Rev. D96 (2017) 9, 094026

2nd Forward Physics Facility Meeting, 27th-28th May 2021, online via ZOOM

Motivation from the Neutrino Astronomy

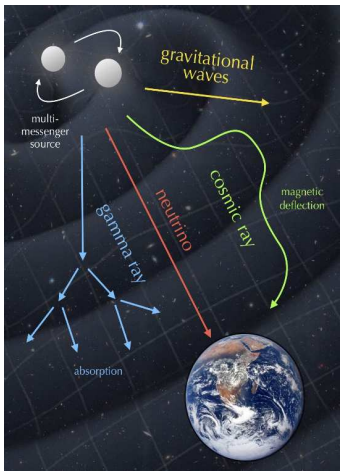

High-energy cosmic neutrinos ⇒ excellent cosmic messenger particles

- Universe not transparent to extragalactic photons with $E_\gamma > 10$ TeV (gamma rays) ⇒ strongly absorbed by interactions with the cosmic microwave background (CMB).
- Neutrinos ⇒ no absorption and no deflection by magnetic fields
  - essentially no mass and no electric charge, weakly interacting
  - can travel cosmic distances without distortion and can point back to their sources
  - can escape dense astrophysical environments where they are produced

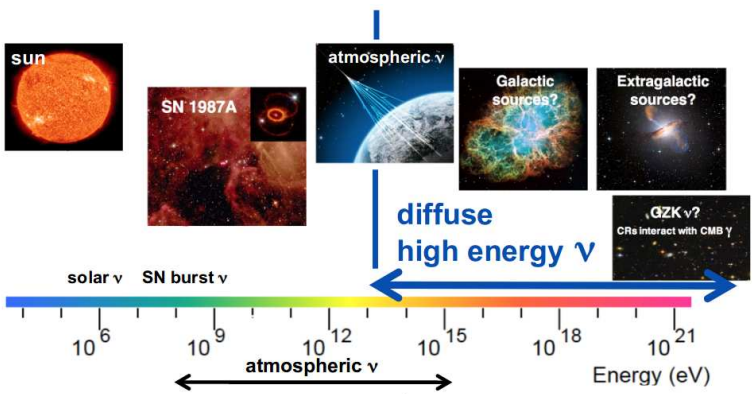

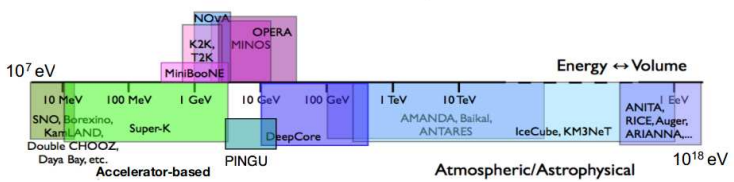

Low-energy extraterrestrial neutrinos

- MeV neutrinos from the Sun (the closet source)
- neutrinos from supernova 1987A

Pushed forward:

- elucidated neutrino properties, neutrino flavor changing puzzle
- fundamental physics, Sun's inner working, supernova physics

- Diffuse high-energy neutrinos ⇒ information about the mechanism of cosmic ray production and cosmic ray sources
  - e.g. probe of the high-energy neutrino-nucleon cross section
  - many new physics phenomena (dark matter, leptoquarks, micro black holes, etc.)

Cosmic Neutrino Detection

Unfortunately, their weak interactions also make cosmic neutrinos very difficult to detect...

- neutrino observatories require gigaton masses ⇒ natural resources needed
- immense detectors to collect cosmic neutrinos in statistically significant numbers
  - first efforts ⇒ a large volume of deep natural water (DUMAND, ANTARES, KM3NeT, BGVD)
  - next steps ⇒ a large volume of transparent natural Antarctic ice (AMANDA and IceCube)

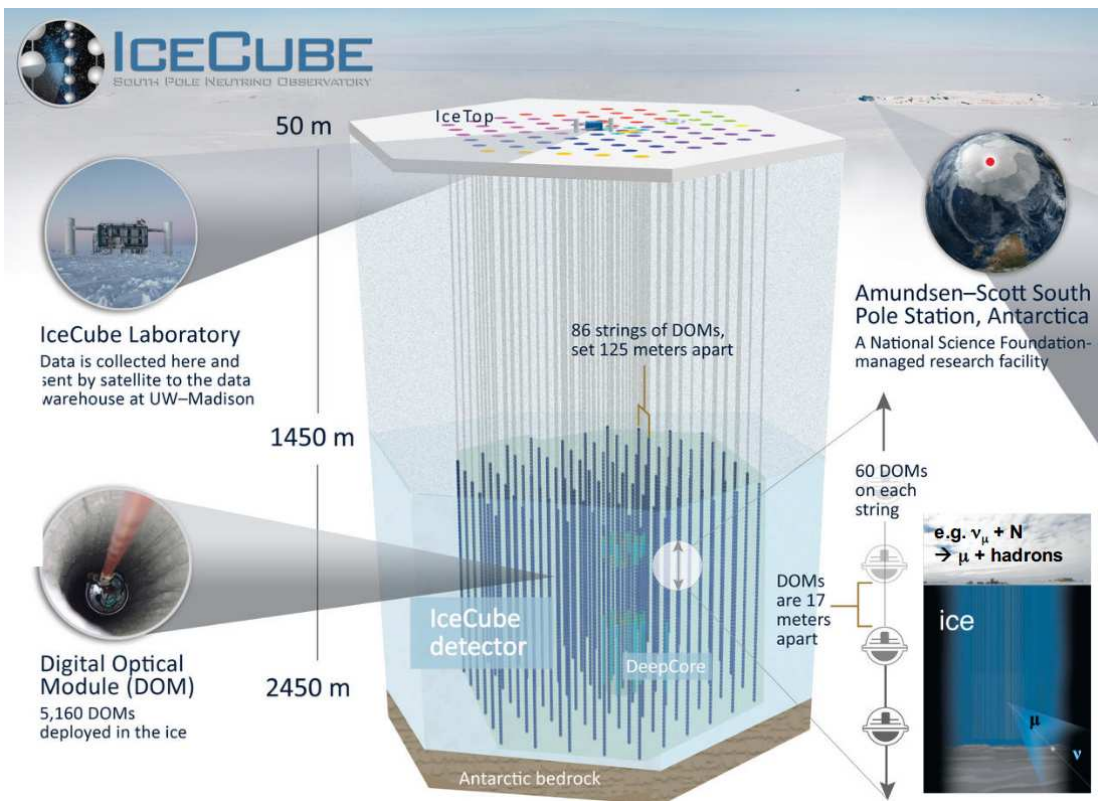

The IceCube Neutrino Observatory

- at the Amundsen–Scott South Pole Station in Antarctica
- an in-ice array (IceCube detector)
- a surface air shower array (IceTop)
- detector medium ⇒ one cubic kilometre of the deep ultra-clear glacial ice

Backgrounds

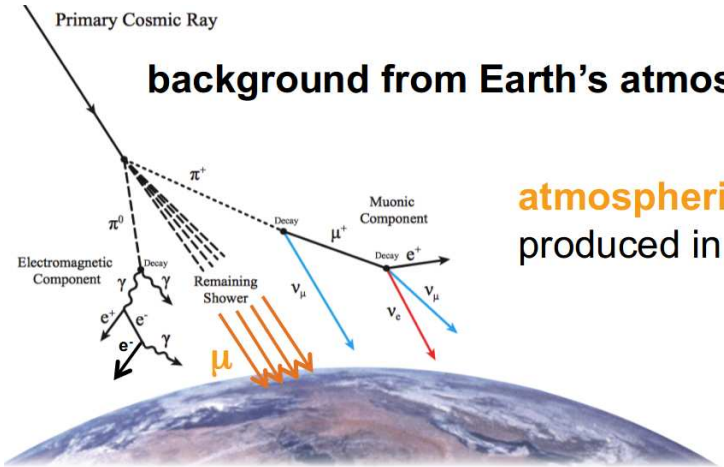

background from Earth's atmosphere

atmospheric muons
produced in cosmic ray air showers

1/10⁶

atmospheric neutrinos
produced in the same showers

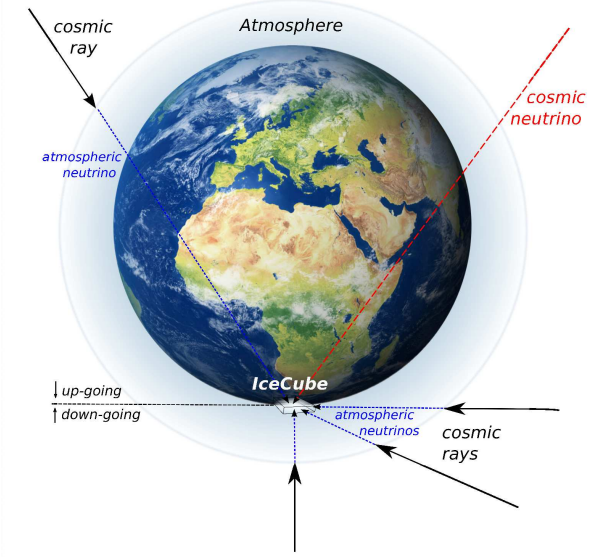

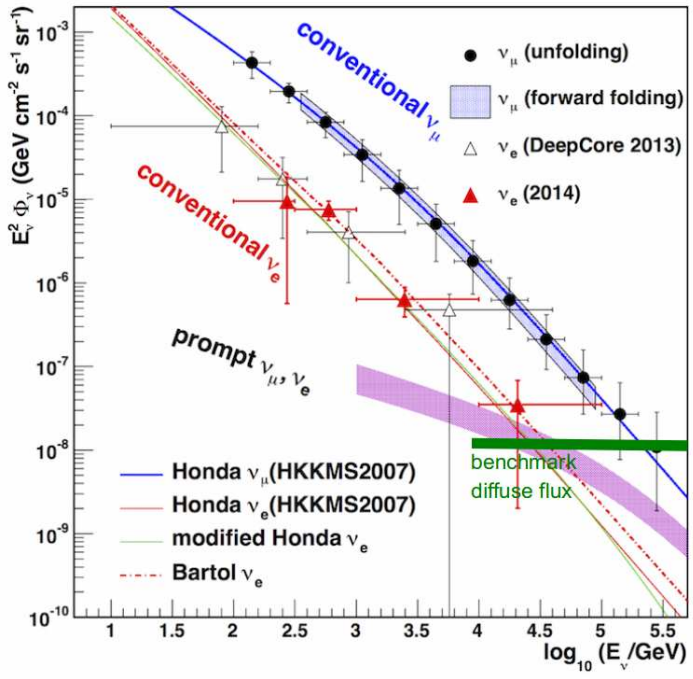

- **conventional** ν-flux $\Rightarrow \Phi_\nu \sim E_\nu^{-3.7}$
  - ▷ decays of lighter mesons: $\pi^\pm$, $K^\pm$
  - ▷ long life-time: interactions occurs before decay
  - ▷ mesons loose energy $\rightarrow$ steeply falling ν-flux
  - ▷ zenith-angle dependent, largest at horizon

- **prompt** ν-flux (not yet identified) $\Rightarrow \Phi_\nu \sim E_\nu^{-2.7}$
  - ▷ decays of heavy mesons: D and B
  - ▷ short life-time: decay before interactions
  - ▷ more energy transferred to neutrino $\rightarrow$ flat ν-flux
  - ▷ isotropic

From cosmic ray to prompt neutrino flux detection

Theoretical predictions of the prompt atmospheric neutrino flux at the detector level $\Rightarrow$

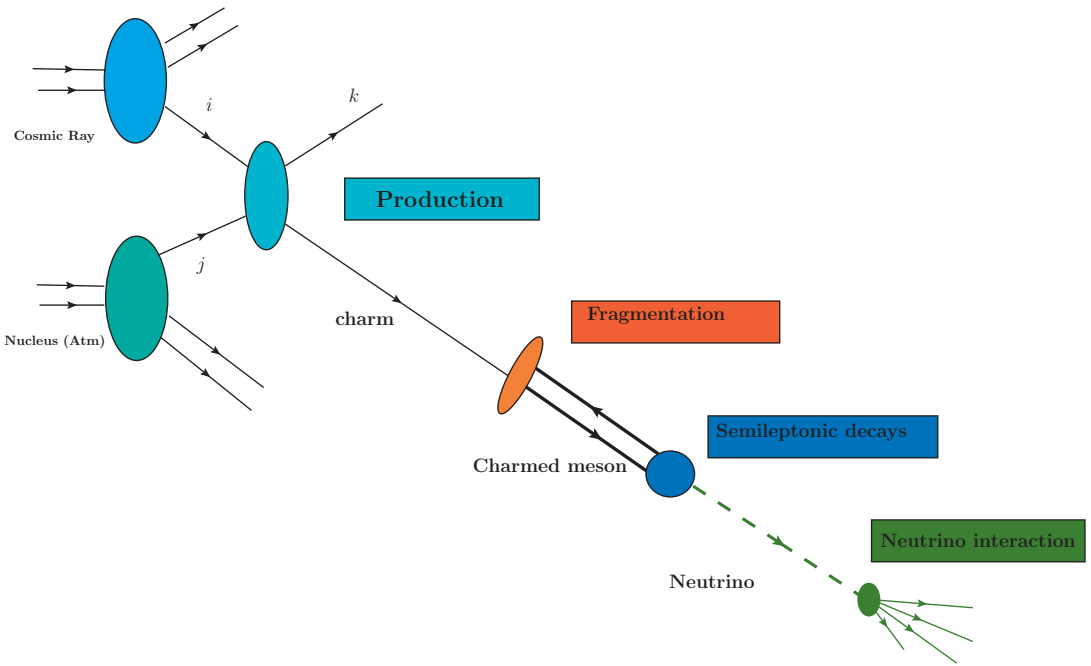

- a multi-stage problem with many sources of uncertainties
  - ▷ **the initial cosmic ray flux**: shape and composition
  - ▷ **strong interaction cross section**: charm production, framework, parton densities, nucelar effects, intrinsic charm
  - ▷ **charm hadronization**
  - ▷ **semileptonic decay**
  - ▷ **neutrino interaction cross section**

high-energy prompt neutrinos ($E_\nu > 10^5$ GeV)
$\Rightarrow$ **high energy limit and far-forward charm meson production**

- QCD methods for the charmed meson production in the kinematics beyond the LHC
  - validity of the collinear factorization in the forward kinematics
  - the size of subleading fragmentation of light partons into heavy meson
  - the presence (or not) of intrinsic heavy quarks in the hadronic wave function
  - the presence (or not) of nonlinear (saturation) effects

Forward charm production at the LHC

Open charm LHCb data in pp-scattering at $\sqrt{s}$ =7, 13 TeV:

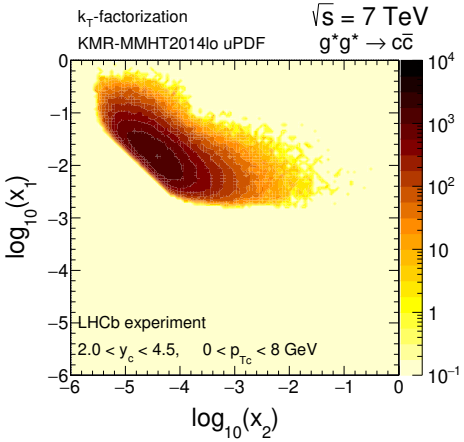

Detector acceptance: $2.0 < y < 4.5$ and $0 < p_T < 8$ GeV

- inclusive D-meson spectra and $D\overline{D}$-pair correlation observables (M_{inv}, $\Delta\varphi$, p_T-pair)
- longitudinal momentum fractions probed: $10^{-3} < x_1 < 10^{-1}$ and $10^{-5} < x_2 < 10^{-3}$
- p_T-differential cross section well described in different y-bins
- correct shapes of the correlation observables

(R.M., A. Szczurek, Phys.Rev.D 100 (2019) 5, 054001)

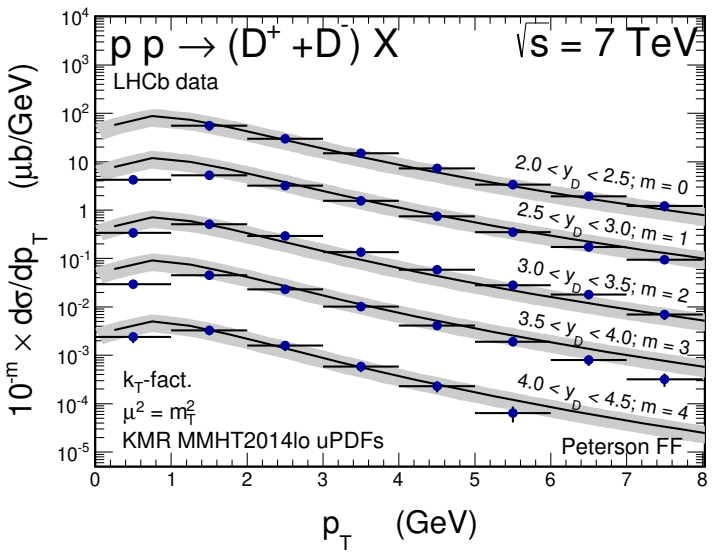

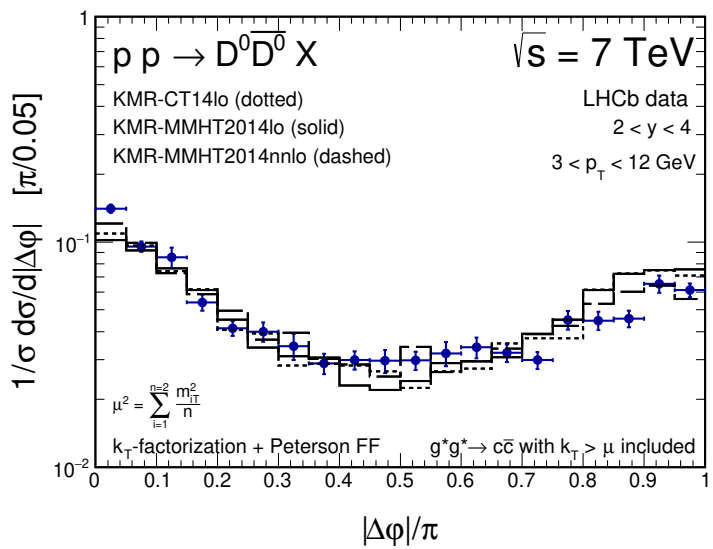

- k_T-factorizaton: $g^*g^* \to c\bar{c}$ + KMR uPDF ⇒ works very well

Kinematics probed with the IceCube prompt neutrino flux

Mapping the dominant regions of the phase space associated with $c\bar{c}$-pair production relevant for the **prompt flux at IceCube**

(V.P. Goncalves, R.M., R. Pasechnik, A. Szczurek, Phys.Rev.D 96 (2017) 9, 094026)

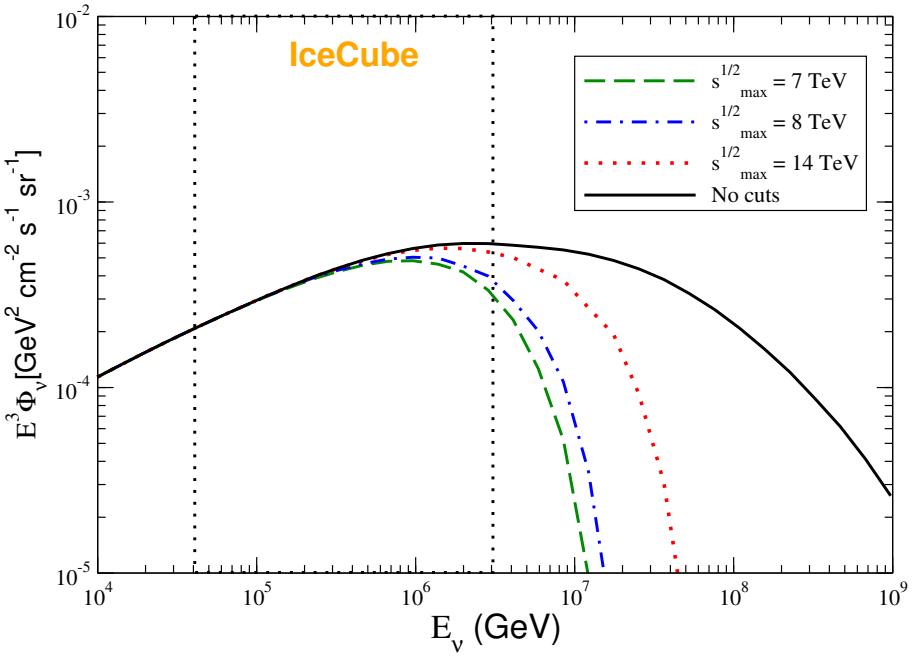

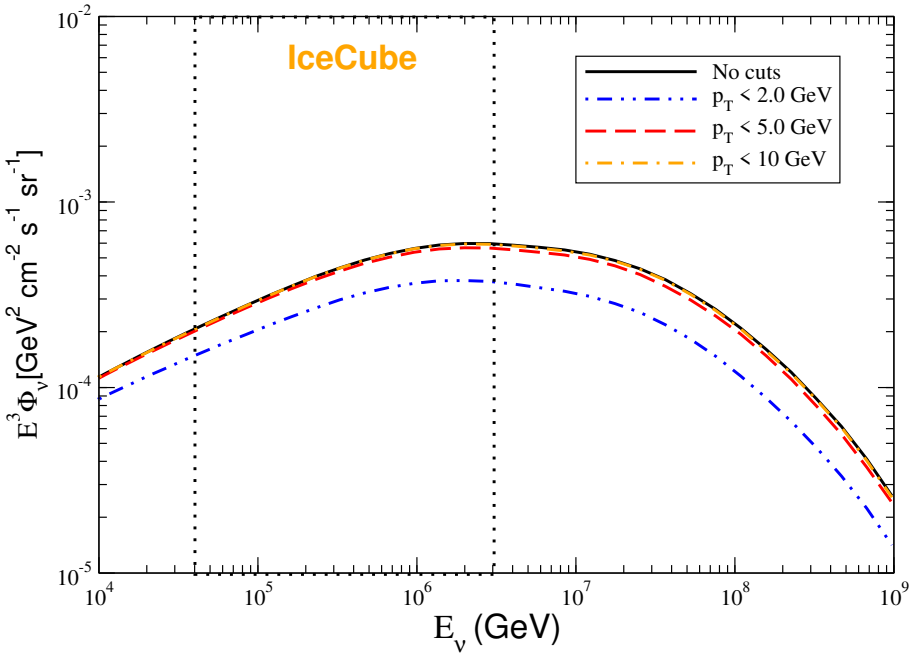

- recent: up to $E_\nu = 3 \cdot 10^6$ GeV $\Rightarrow$ **the LHC energy range**
- future: $E_\nu > 10^7$ GeV $\Rightarrow$ energy range beyond that probed in the LHC Run2
- flux sensitive to the $p_T < 5$ GeV

Kinematics probed with the IceCube prompt neutrino flux

Mapping the dominant regions of the phase space associated with $c\bar{c}$-pair production relevant for the **prompt flux at IceCube**

(V.P. Goncalves, R.M., R. Pasechnik, A. Szczurek, Phys.Rev.D 96 (2017) 9, 094026)

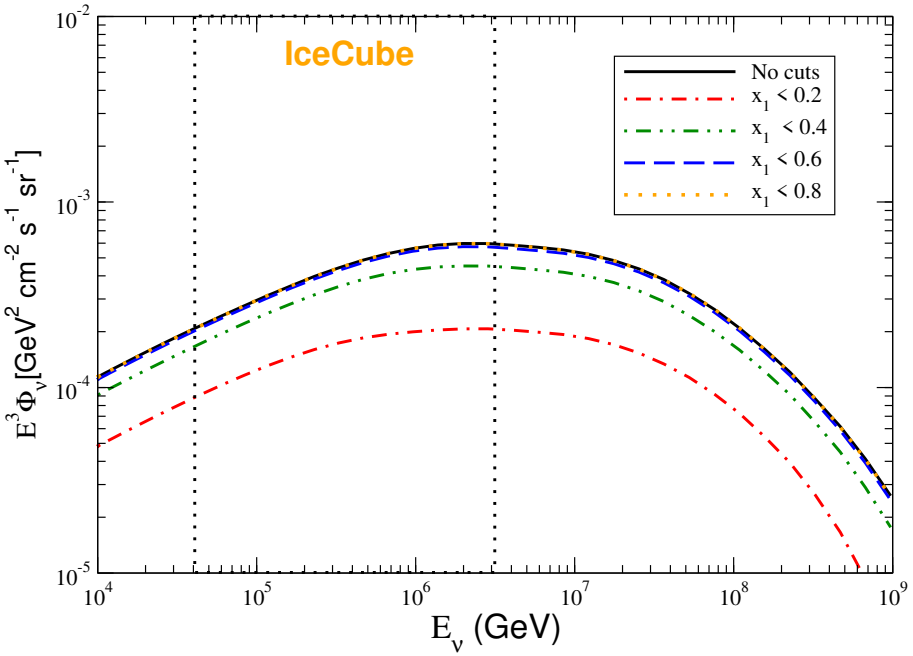

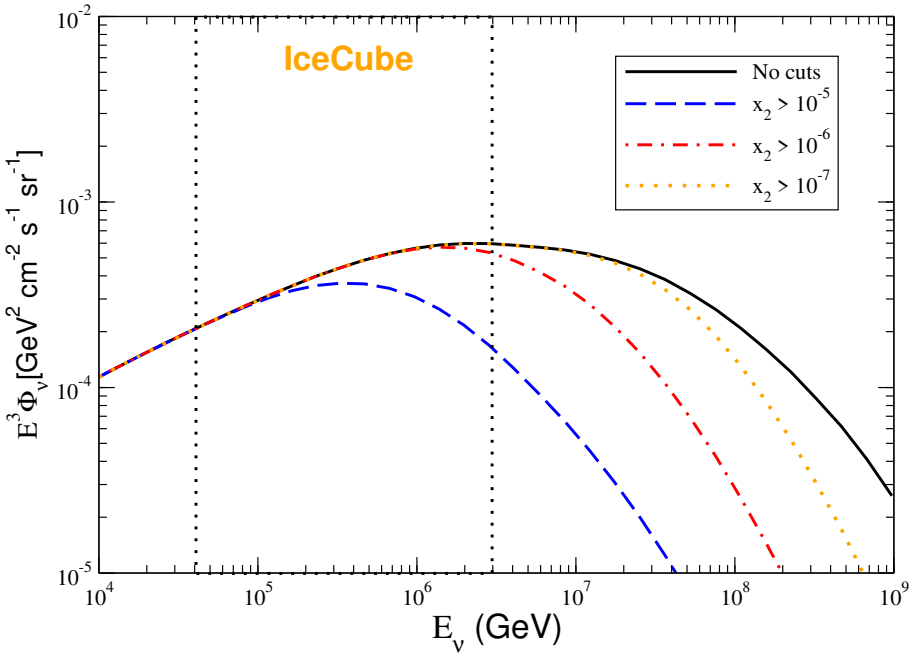

- projectile: $0.2 < x_1 < 0.6$
- target: $10^{-6} < x_2 < 10^{-5}$ (IceCube recently) and even $10^{-8} < x_2 < 10^{-5}$ (future)
- **far-forward production beyond the LHC range** $\Rightarrow$ very asymmetric kinematics

Hybrid high-energy factorization

How to treat theoretically the asymmetric configuration?

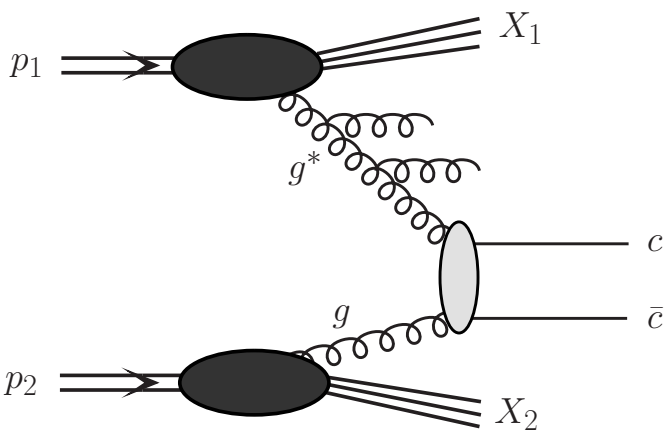

The hybrid approach for far-forward production $\Rightarrow$

- combined collinear- and k_T-factorization
- used in many phenomenological studies
- the differential cross section for $gg^* \to c\bar{c}$ mechanism:

$$d\sigma_{pp\to charm}(gg^* \to c\bar{c}) = \int dx_1 \int \frac{dx_2}{x_2} \int d^2k_t \times g(x_1,\mu^2)\cdot \mathcal{F}_g(x_2,k_t^2,\mu^2)\cdot d\hat{\sigma}_{gg^*\to c\bar{c}}$$

- $g(x_1,\mu^2)$ $\Rightarrow$ collinear large-x gluon (the one from the incoming cosmic ray)
  we use the CT14nnlo PDF
- $\mathcal{F}_g(x_2,k_t^2,\mu^2)$ $\Rightarrow$ off-shell small-x gluon (the one from the target air nucleus)
  we use the KMR/MRW and the KS linear/nonlinear uPDFs
- $d\hat{\sigma}_{gg^*\to c\bar{c}}$ is the hard partonic cross section obtained from a gauge invariant off-shell tree-level amplitudes (available in KaTie)
- the hybrid model used in the past in the context of prompt neutrino flux at IceCube:
  Bhattacharya, Enberg, Jeong, Kim, Reno, Sarcevic, Stasto, JHEP 11 (2016) 167
  but only for gluon-gluon channel (no intrinsic charm there)

Charm production driven by the intrinsic charm

NEW in our study:

- for the first time the intrinsic charm contribution to forward charm production and to prompt neutrino flux at IceCube from the exact pQCD calculations
- previous studies based on phenomenological fits to low-energy forward charm data (LEBC-MPS) and their further extrapolation to high energies

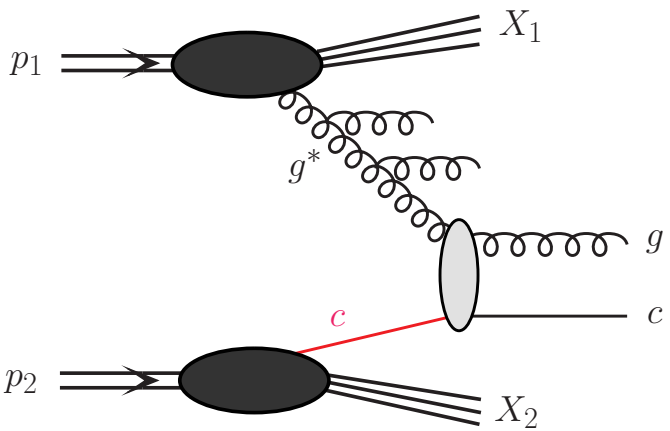

The charm quark in the initial state $\Rightarrow$

- perturbative: extrinsic charm (from gluon splitting)
- non-perturbative: **intrinsic charm (IC)**

$$d\sigma_{pp\to charm}(cg^* \to cg) = \int dx_1 \int \frac{dx_2}{x_2} \int d^2k_t \times c(x_1,\mu^2)\cdot \mathcal{F}_g(x_2,k_t^2,\mu^2)\cdot d\hat{\sigma}_{cg^*\to cg}$$

- $c(x_1,\mu^2)$ $\Rightarrow$ collinear charm quark PDF (large-x)
- $\mathcal{F}_g(x_2,k_t^2,\mu^2)$ $\Rightarrow$ off-shell gluon uPDF (small-x)

- $d\hat{\sigma}_{cg^*\to cg}$ $\Rightarrow$ only in the massless limit (also available in KaTie)
- regularization needed at $p_T \to 0$ $\Rightarrow$ we use PYTHIA prescription:
  $F_{sup}(p_T) = \frac{p_T^2}{p_{T0}^2+p_T^2}$, $\alpha_S(\mu_R^2 + p_{T0}^2)$, where $p_{T0} = 1.5$ GeV (free parameter)
- the charm quark PDF with IC content is taken at the initial scale: $c(x_1,\mu_0^2)$, where $\mu_0 = 1.3$ GeV so the perturbative charm contribution is intentionally not taken into account

The concept of intrinsic charm in the nucleon

The intrinsic charm quarks ⇒ multiple connections to the valence quarks of the proton

- strong evidence for internal strangeness and somewhat smaller for internal charm

- global experimental data put only loose constraints on the P_{ic} probability
- dfferent pictures of non-perturbative $c\bar{c}$ content:
  - sea-like models
  - valence-like models
- we use the IC distributions from the Brodsky-Hoyer-Peterson-Sakai (BHPS) model as adopted in the CT14nnloIC PDF

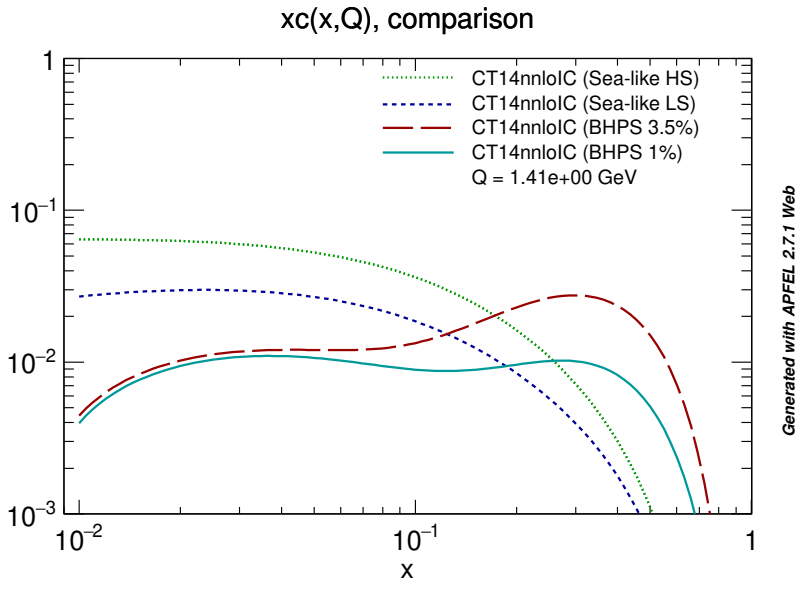

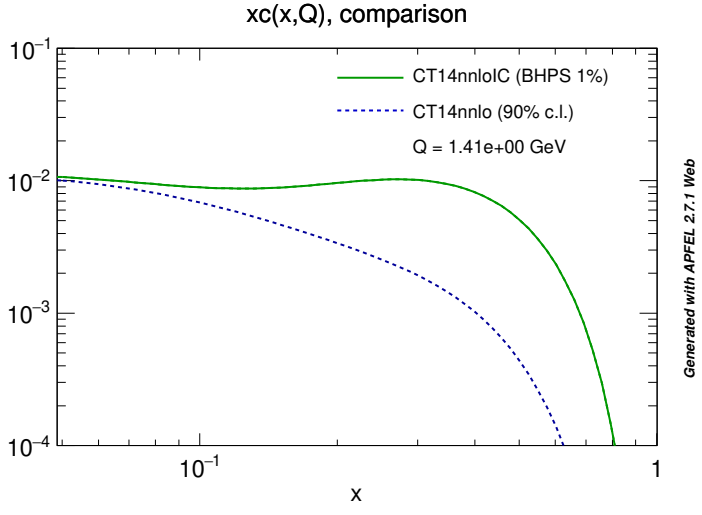

- the presence of an intrinsic component implies a large enhancement of the charm distribution at large x (>0.1) in comparison to the extrinsic charm prediction
- the models do not allow to predict precisely the absolute probability P_{ic}

Intrinsic charm at the LHC and beyond

A possible impact of the intrinsic charm component on the forward charm particle production in already existing or future experiments at different energies:
(R.M, A. Szczurek, JHEP 10 (2020) 135)

- Future Circular Collider (FCC) (D-meson production)

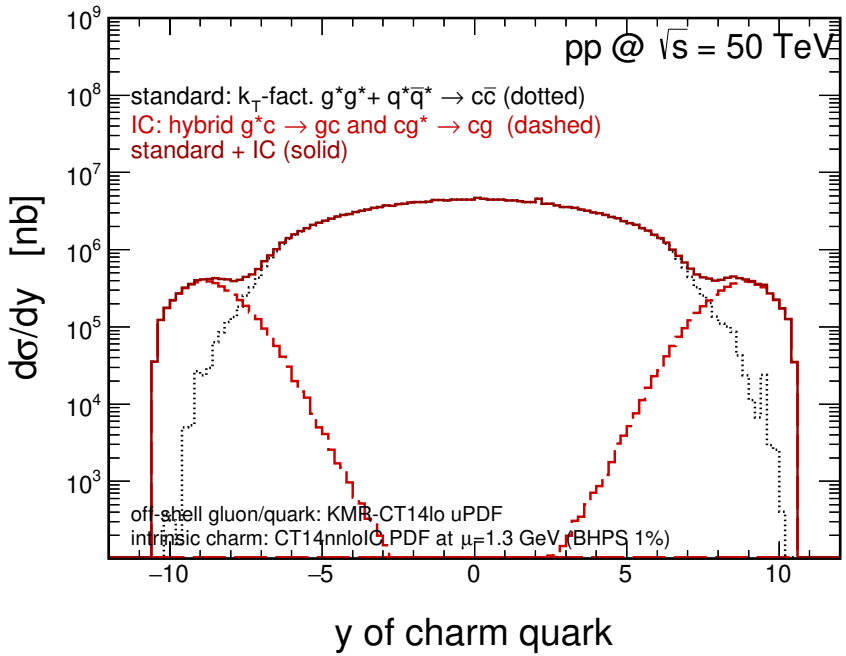

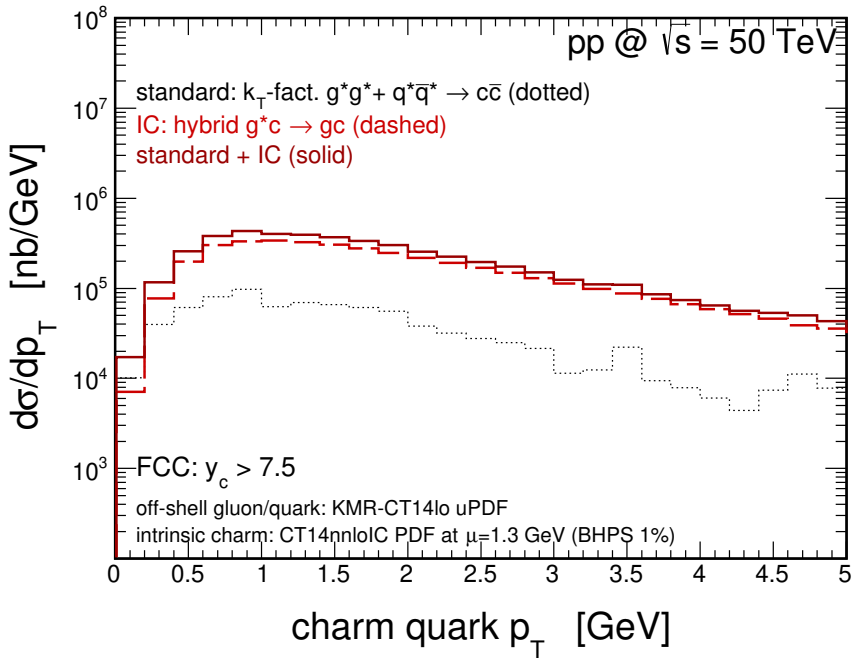

- the intrinsic charm important at $|y| > 7$
- transverse momentum distribution visibly enhanced

Intrinsic charm at the LHC and beyond

A possible impact of the intrinsic charm component on the forward charm particle production in already existing or future experiments at different energies:

(R.M, A. Szczurek, JHEP 10 (2020) 135)

- FASER at the LHC (dedicated to a measurement of forward neutrinos originating from semileptonic decays of D mesons)

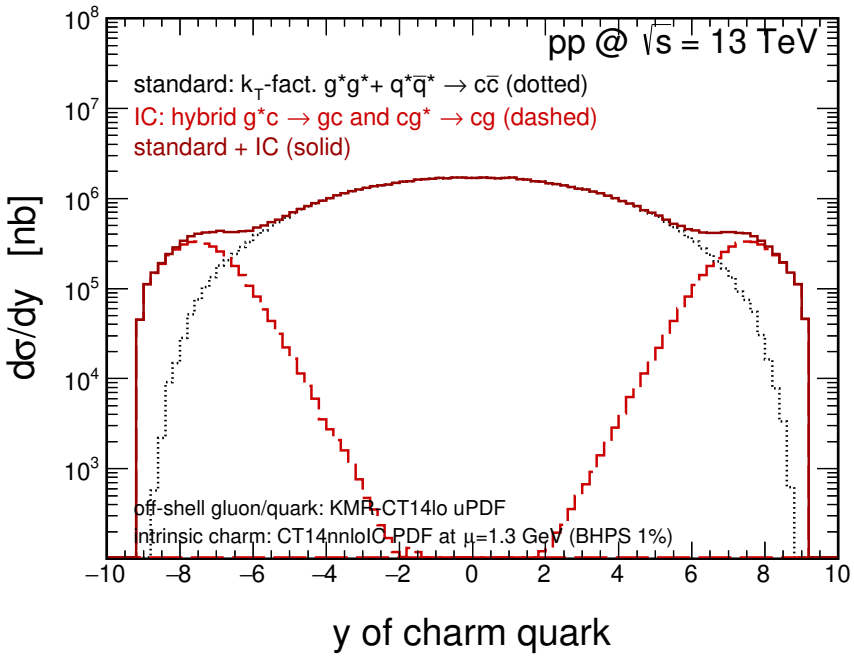

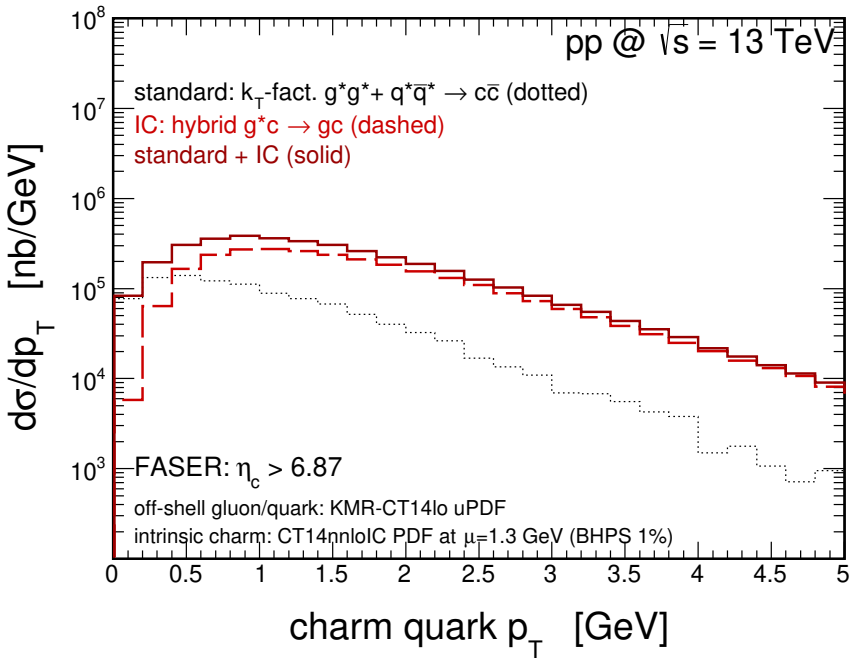

- the intrinsic charm important at $|y| > 6$
- transverse momentum distribution visibly enhanced

Intrinsic charm at the LHC and beyond

A possible impact of the intrinsic charm component on the forward charm particle production in already existing or future experiments at different energies:

(R.M, A. Szczurek, JHEP 10 (2020) 135)

- SHIP at the SPS CERN at $\sqrt{s} = 27.4$ GeV (dedicated to a measurement of forward ν_τ neutrinos originating from semileptonic decays of D_s mesons)

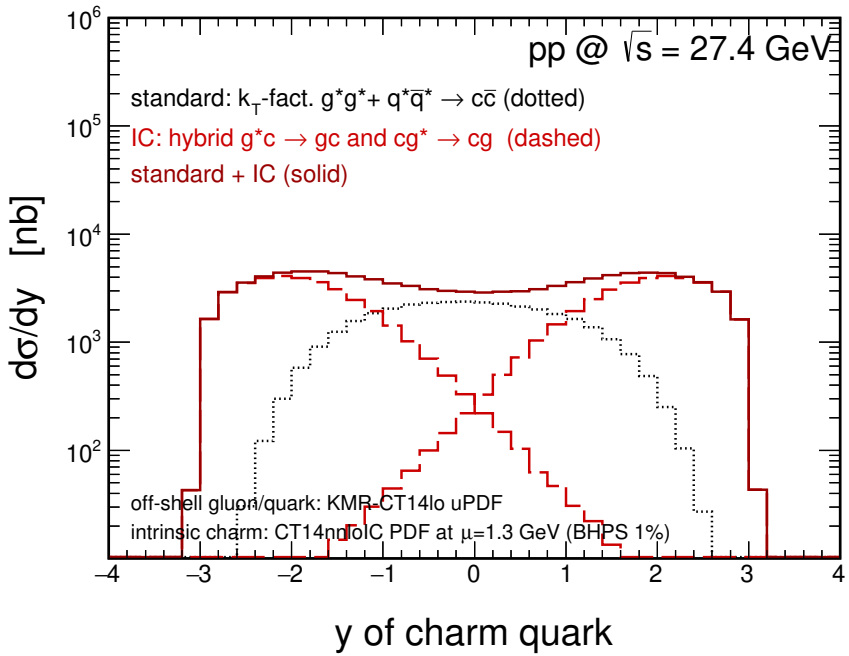

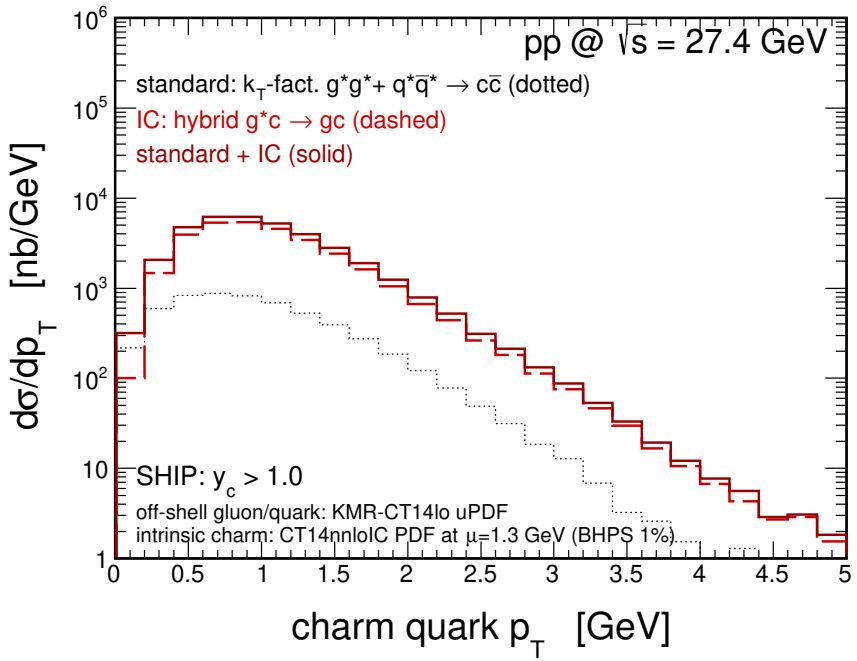

- at the lower energy ⇒ the intrinsic charm important in the whole rapidity spectrum
- transverse momentum distribution visibly enhanced

Intrinsic charm at the LHC and beyond

A possible impact of the intrinsic charm component on the forward charm particle production in already existing or future experiments at different energies:
(R.M, A. Szczurek, JHEP 10 (2020) 135)

- Fixed-target LHCb mode at $\sqrt{s} = 86.6$ GeV (D-meson production)

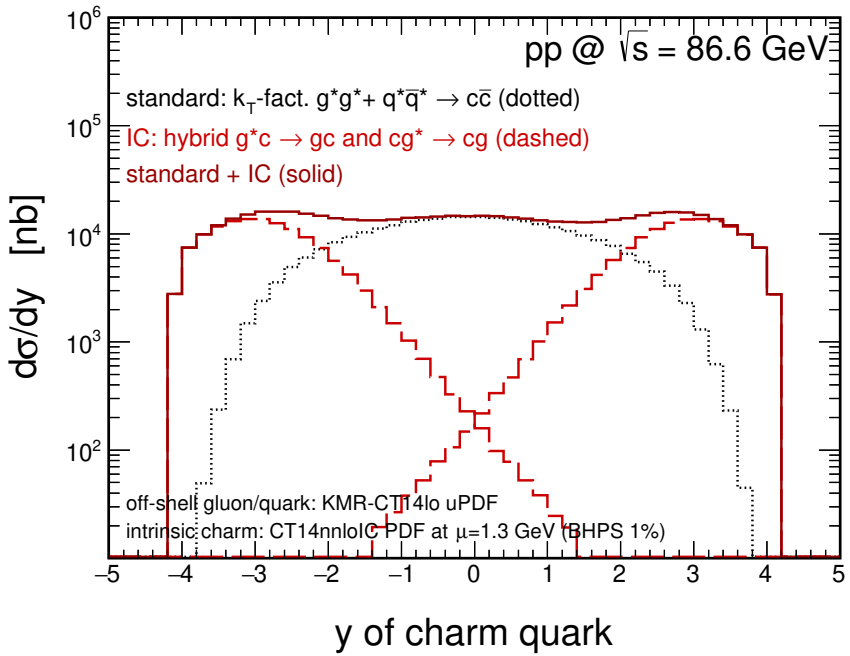

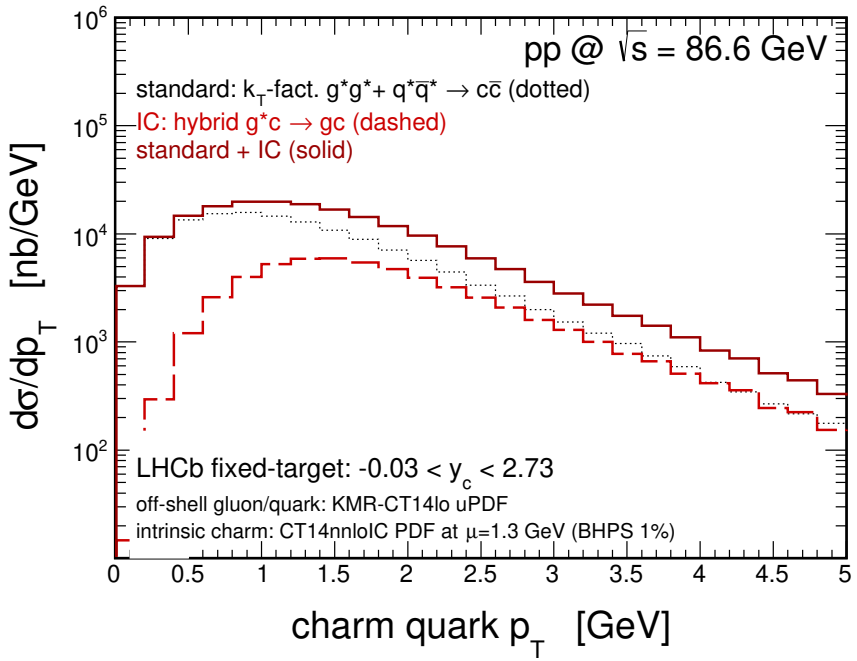

- at the lower energy $\Rightarrow$ the intrinsic charm important already at $|y| > 1$

Intrinsic charm at the LHC and beyond

The fixed-target data on forward open charm meson production already exists:

- Fixed-target LHCb mode at $\sqrt{s} = 86.6$ GeV (D-meson production)

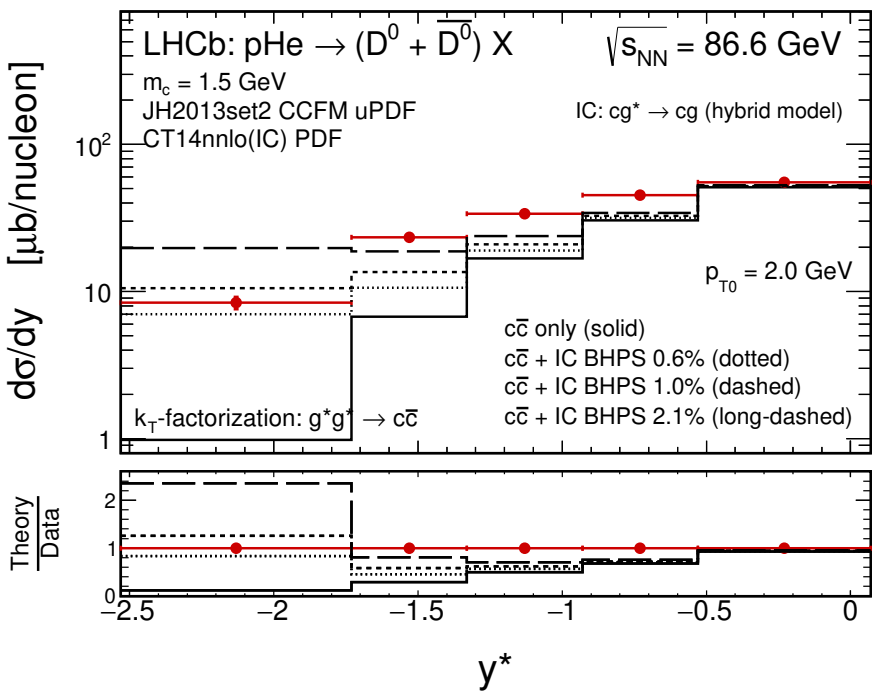

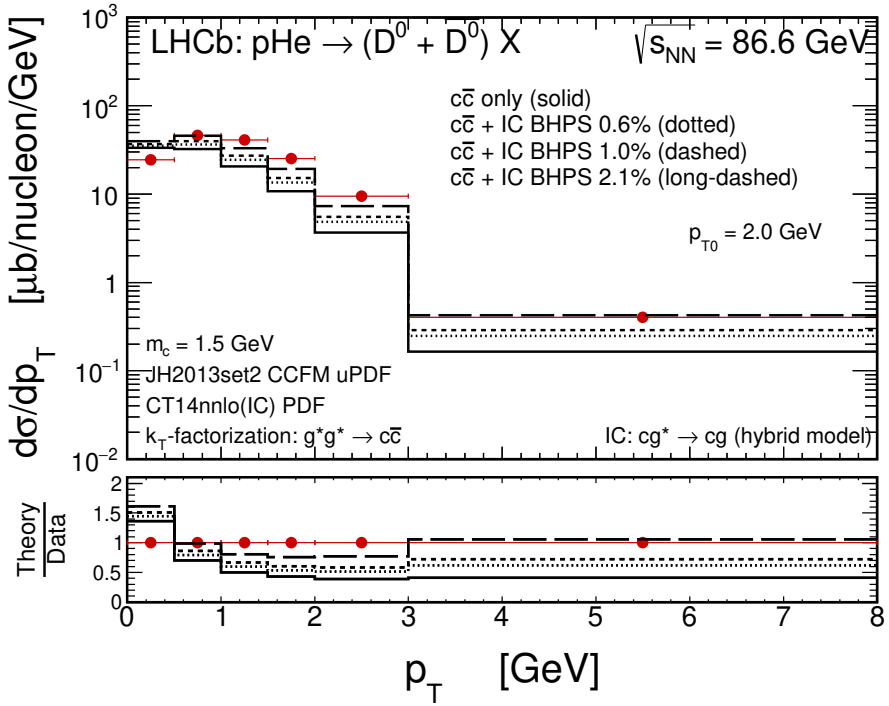

- some problems with understanding the LHCb fixed-target open charm data identified (R.M., Phys.Rev.D 102 (2020) 1, 014028)
- a new scenario proposed with the intrinsic charm contribution needed to describe the data points in the backward direction and at larger p_T's
- R.M, A. Szczurek, arXiv:2105.09370 [hep-ph]

Intrinsic charm at the LHC and beyond

The older fixed-target data on forward open charm meson production:

- LEBC-MPS at $\sqrt{s} = 38.7$ GeV (D-meson production)

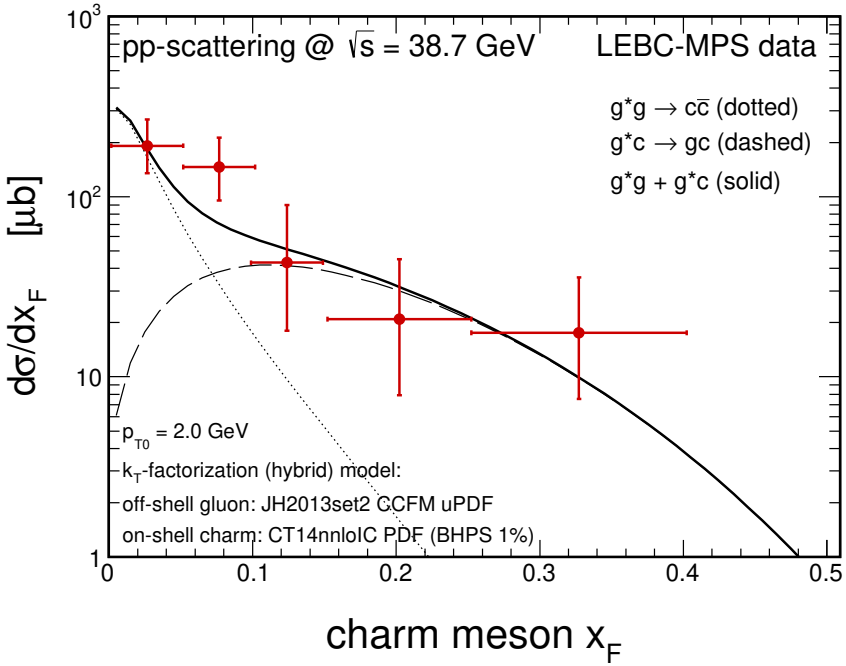

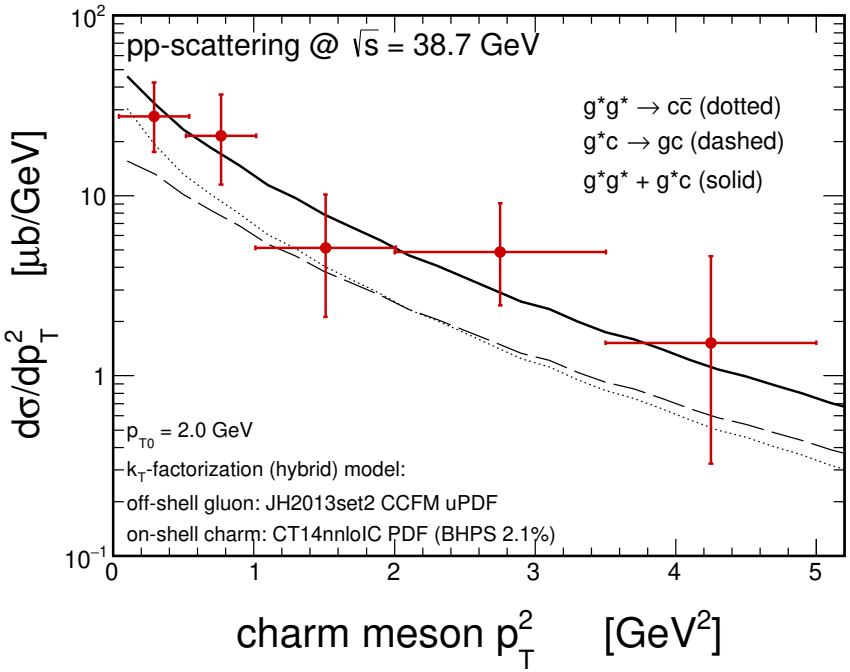

- the data well described with the same set of parameters as in the LHCb case
- $\frac{d\sigma}{dx_F}(E) \Rightarrow$ exact pQCD calculations here (for different energies)

- Laha-Brodsky in Phys.Rev.D96,(2017) 123002 $\Rightarrow x_F$-distributions from a probability distribution of n-particle $c\bar{c}$ Fock state, fitted to the LEBC-MPS data and extrapolated to high energies (the energy dependence from the parametrization of the pp inelastic cross section, only the normalization changes)
- Halzen-Wille in Phys.Rev.D94, (2016) 014014 $\Rightarrow$ model-independent parametrization for forward charm production (the energy and Feynman-x dependence)

Prompt neutrino fluxes

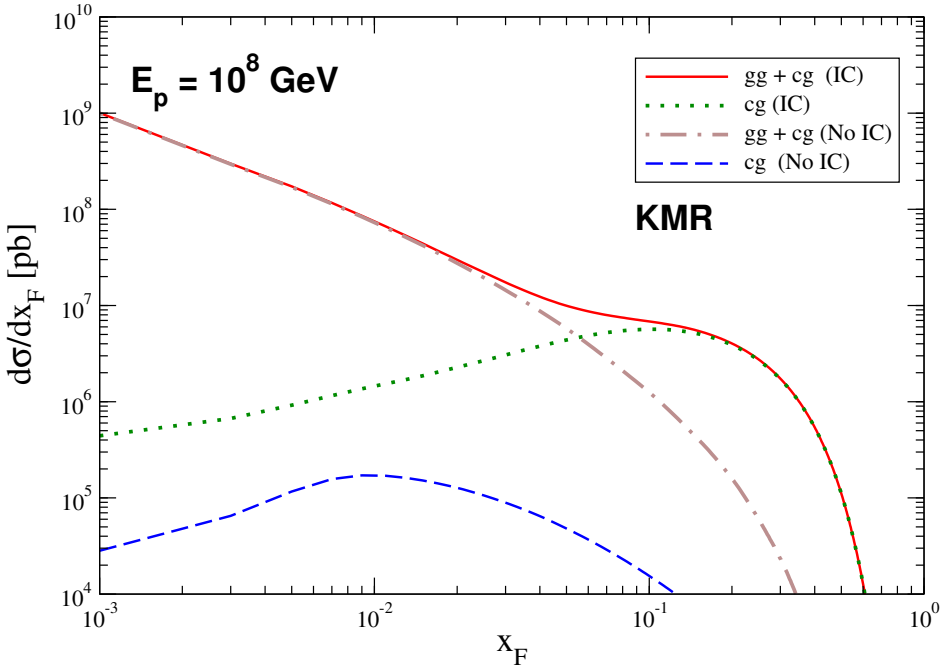

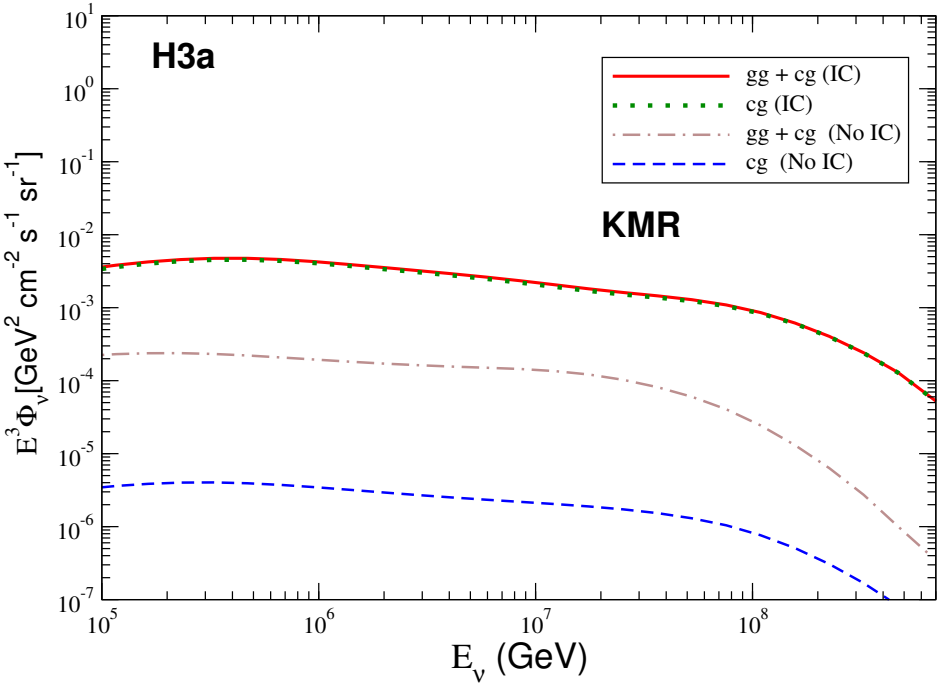

- when intrinsic charm is included the behaviour of the x_F-distribution is strongly modified in the $0.03 \leq x_F \leq 0.6$ range
- the Feynman x_F-distribution for large x_F is dominated by the $cg^* \to cg$ mechanism
- extrinsic charm negligible

- the inclusion of the $cg^* \to cg$ mechanism driven by the intrinsic charm (IC) has a strong effect on the prompt neutrino flux
- the flux is enhanced by one order of magnitude when intrinsic charm is present ($P_{ic} = 1\%$ here)

Predictions and IceCube limits for intrinsic charm

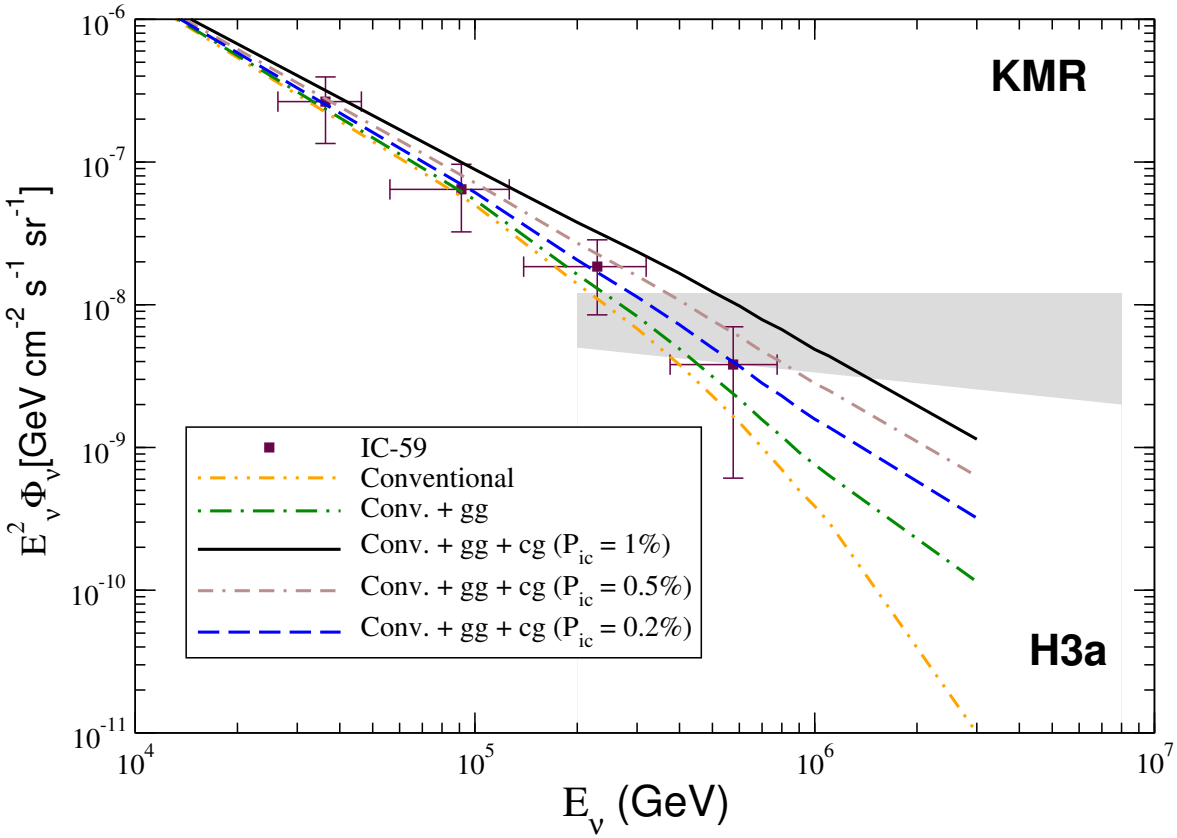

- the impact of the prompt flux is small in the current kinematical range probed by IceCube as long as only the gluon-gluon fusion mechanism is taken into account
- the intrinsic charm mechanism implies a large enhancement of the prompt flux at large E_ν, with the associated magnitude being strongly dependent on the value of P_{ic}
- linear QCD dynamics $\Rightarrow P_{ic} \leq 0.5\%$

Predictions and IceCube limits including saturation

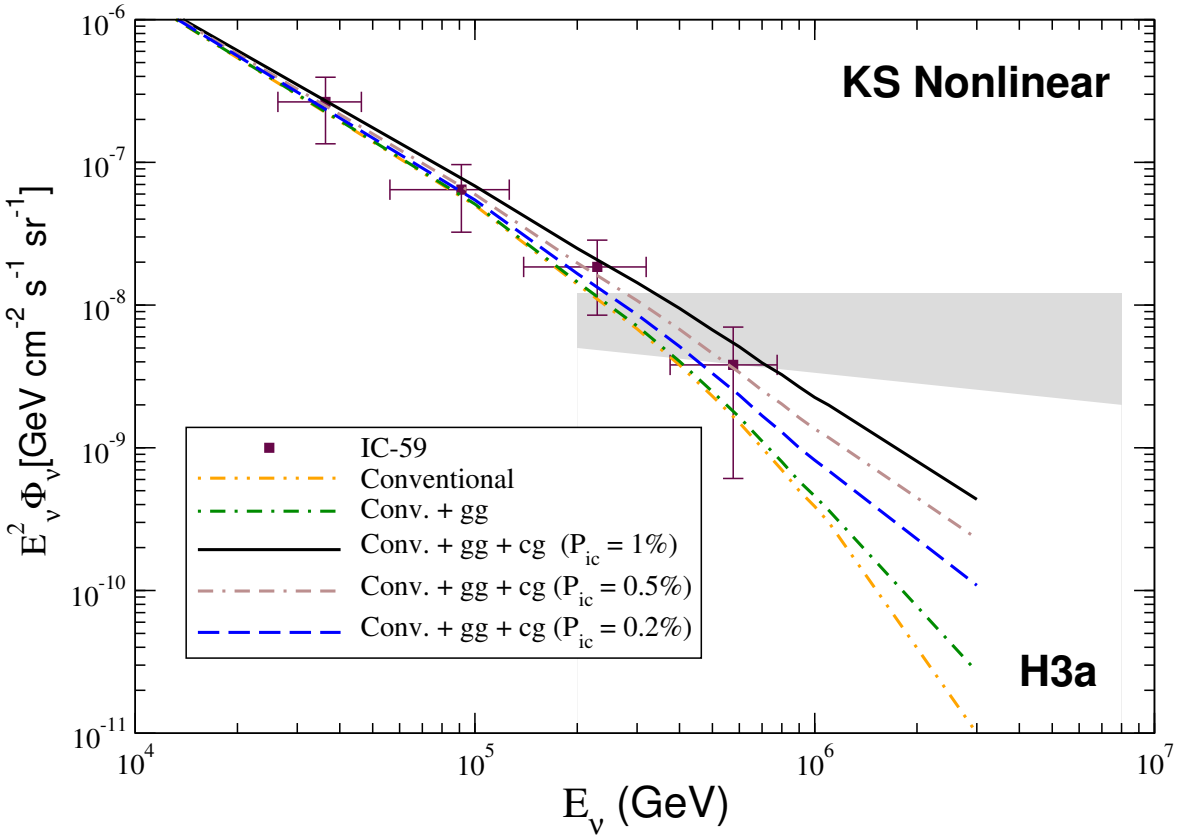

- within the saturation scenario the impact of the prompt flux driven by the gluon-gluon fusion mechanism is even smaller and becomes negligible
- nonlinear QCD dynamics $\Rightarrow$ $P_{ic} \leq 1.0\%$
- consistent with the central CT14nnloIC PDF set

Conclusions

Currently we have two acceptable solutions when the intrinsic charm mechanism is included in the analysis of the IceCube prompt neutrino flux:

- the QCD dynamics is described by a linear evolution equation and the amount of IC in the proton wave function has the upper limit $P_{ic} \leq 0.5\%$ that is smaller than the value predicted by the central CT14nnloIC parameterization
- the amount of IC at the level of about 1.0% is correctly described by the central CT14nnloIC parameterization and the saturation effects are needed to describe the IceCube prompt neutrino flux at the highest energies rapidities

One has that if the amount of IC is constrained in hadronic colliders, the IceCube data for the atmospheric neutrino flux can be considered as a probe of the QCD dynamics at high energies. Inversely, if the saturation effects are probed in hadronic colliders, the IceCube data can be used to constrain the amount of the IC. Such results demonstrate synergy between IceCube and the LHC, and strongly motivate new experimental and theoretical analyses in the future.

- one of such alternatives is the analysis of the D-meson and ν_μ neutrino at FASER taking into account both effects, which we intend to study in a forthcoming publication

Thank You!

BackUp slides

(just in case)

IceCube Detector

The detector volume is instrumented with:

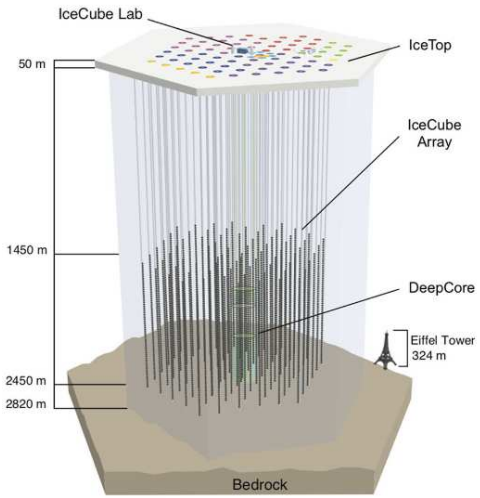

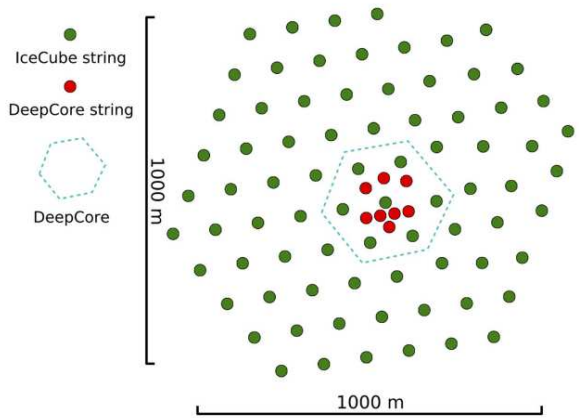

- 5160 Digital Optical Modules (DOMs)
- distributed on 86 read out and support cables ("strings")
- deployed between 1.5 and 2.5 km below the surface
- neutrino energy threshold about 10 GeV

The DOMs register the Cherenkov light emitted by relativistic charged particles passing through the detector

- Cherenkov light is emitted when particle velocity exceeds the speed of light in the given medium
- it is emitted by a charged particle: either prompt (like atm. muons) or resulting from neutrino interaction with ice or bedrock

Cherenkov angle: $\cos\theta_c = 1/(\beta n)$, $\theta_c = 42^\circ$ *water*

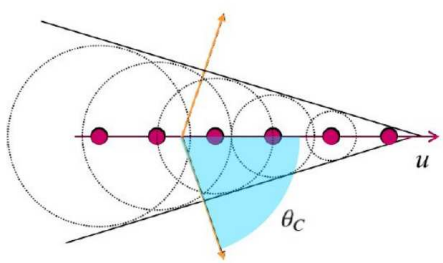

IceCube facility and review of particle physics: M. Ahlers, K. Helbing, C. Heros, Eur. Phys. J. C (2018) 78, M. Ahlers, F. Halzen, Progress in Particle and Nuclear Physics 102 (2018) 73-88

Experimental signatures

There are two principle classes of Cherenkov events (red early in time, blue late in time):

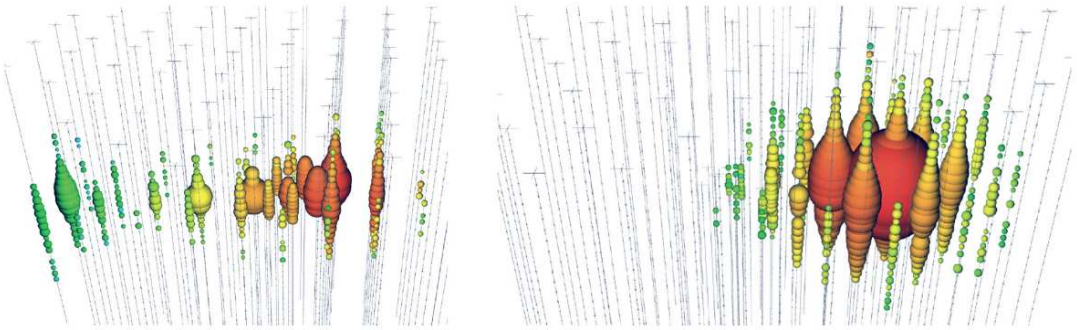

Fig. 2 Two examples of events observed with IceCube. The left plot shows a muon track from a ν_μ interaction crossing the detector. Each coloured dot represents a hit DOM. The size of the dot is proportional to the amount of light detected and the colour code is related to the relative timing of light detection: read denotes earlier hits, blue, later hits. The right plot shows a ν_e or ν_τ charged-current (or any flavour neutral-current) interaction inside the detector

- **TRACKS**: through-going track-like pattern (left panel)
- **CASCADES**: spherical light distribution (right panel)
- starting tracks (cascade + track)

- CC: $\nu_\mu + N \rightarrow \mu +$ hadrons (tracks)

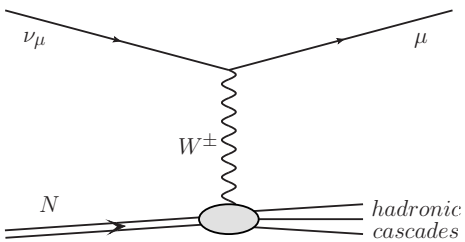

- CC: $\nu_e + N \rightarrow e +$ hadrons (cascades)

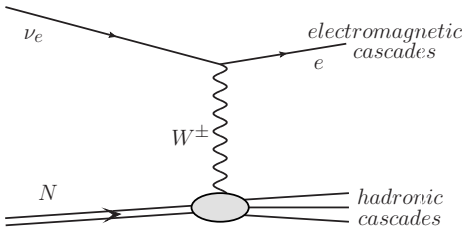

- CC: $\nu_\tau + N \rightarrow \tau +$ hadrons (double cascades)

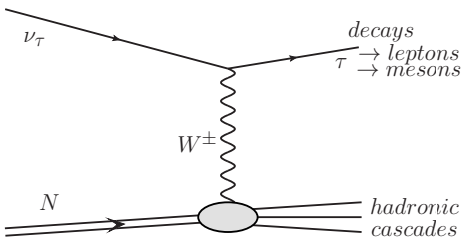

- NC: $\nu_\alpha + N \rightarrow \nu_\alpha +$ hadrons (cascades)

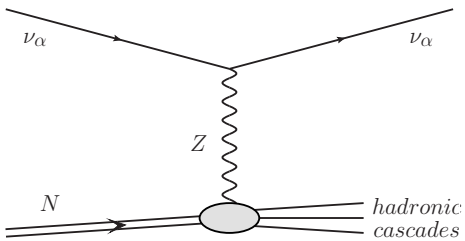

How to reduce the atmospheric background?

Two complementary strategies:

- ν_μ tracks from Northern Sky
  - ▷ using the Earth as a filter by selecting up-going track events
  - ▷ atm. muons sufficiently reduced
  - ▷ vertex outside the detector
- Starting Events (HESE, $E_\nu \gtrsim 30$ TeV)
  - ▷ high-energy ν interacting inside the detector
  - ▷ all directions in the sky
  - ▷ a virtual veto region
  - ▷ rejects atmospheric muons and neutrinos

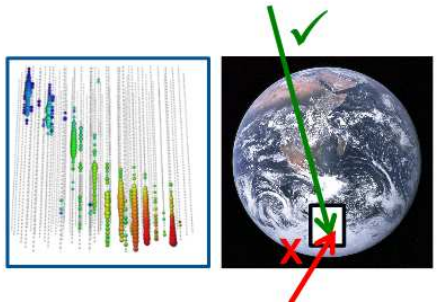

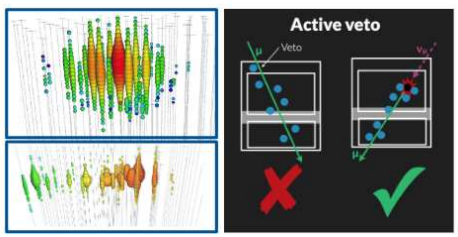

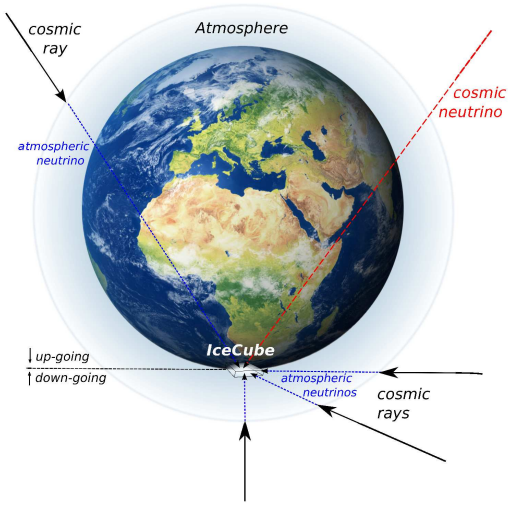

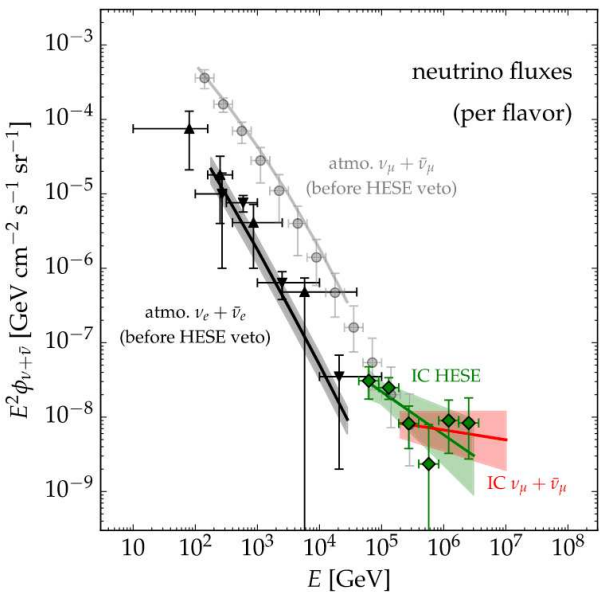

- HESE veto data ⇒ the first observation of high-energy astrophysical neutrinos by IceCube (no atmospheric background)
- study of the ν_μ tracks data from Northern Sky (before HESE veto) ⇒ could be use to constrain the prompt atmospheric neutrino flux and physics behind in the kinematical limits beyond the LHC

(IceCube Collaboration, Astrophys. J. 833 (2016))

Initial cosmic ray (CR) flux

The energy spectra of **cosmic rays on top of the Earth atmosphere**

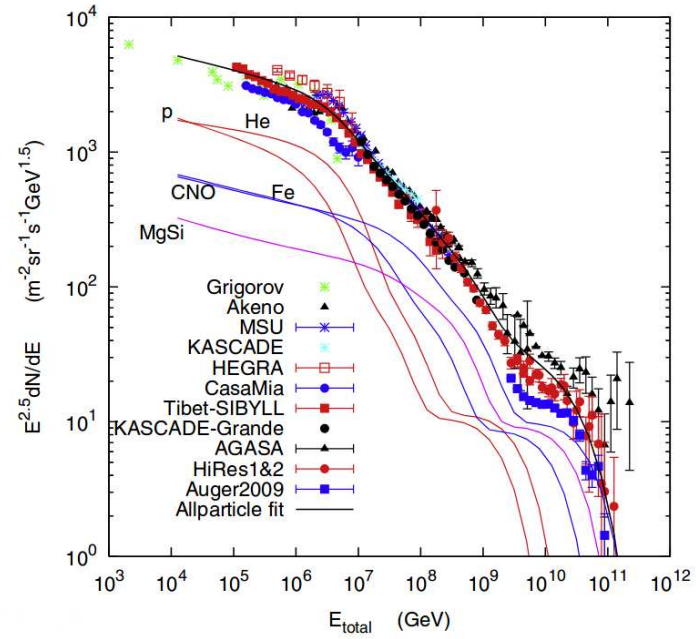

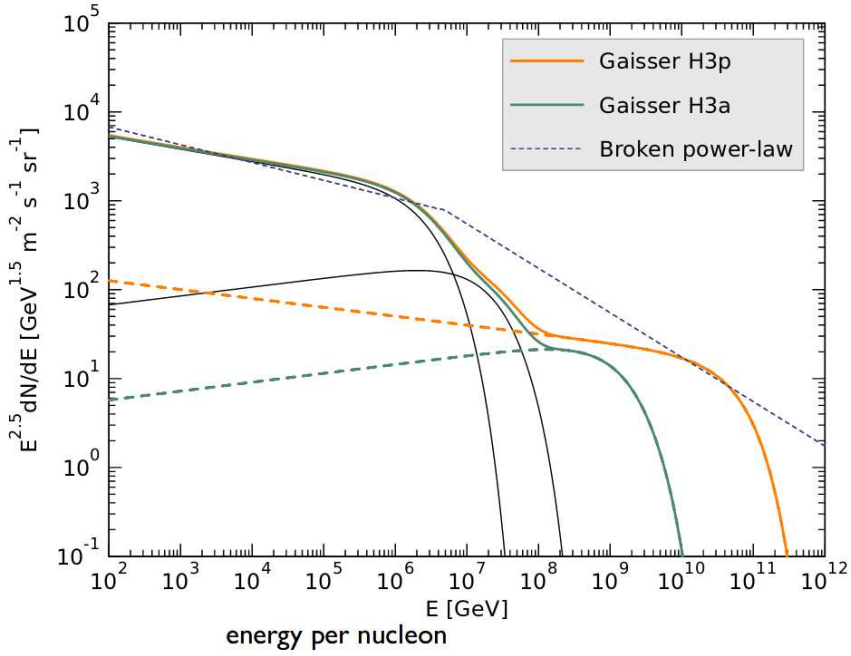

Parametrization by Gaisser

(Gaisser, Astropart. Phys.35, 801 (2012))

$$\phi_i(E) = \sum_{j=1}^{3} a_{i,j} E^{-\gamma_{i,j}} \times \exp[-\frac{E}{Z_i R_{c,j}}]$$

- 5 nuclei groups: H,He,CNO,Fe,MgSi
- 3 populations characterised by different rigidities (1st: supernova remnants, 2nd: higher energy galactic, 3rd: extragalactic component)
- H3a and H3p (only protons in the 3rd pop.)

Broken power-law

$$\phi_p^0(E) = 1.7 E^{-2.7} \text{ for } E < 5 \cdot 10^6 \text{ GeV}$$
$$\phi_p^0(E) = 174 E^{-3} \text{ for } E > 5 \cdot 10^6 \text{ GeV}$$

- used in earlier works
- overestimates the highest energies

Development of air-showers and lepton fluxes

Next step: **Simulation of the propagation of high energy particles and their decay products through the atmosphere**

- The aim is to solve a series of coupled differential equations dependent on **the slant depth** $X(l, \theta)$ measuring the amount of atmosphere traversed by a particle:

$$X(l, \theta) \equiv \int_l^\infty \rho[h(l', \theta)] \mathrm{d}l' \,,$$

  where ρ is the density of the atmosphere dependent on the distance from the ground l (along the particle trajectory) as well as on the zenith angle θ
- an isothermal model of the atmosphere $\Rightarrow$ appropriate for atmospheric depths 10–40 km within which the bulk of particle production occurs:

$$\rho(h) = \rho_0 \exp\left(-h/h_0\right) \,, \quad \rho_0 = 2.03 \times 10^{-3} \ \mathrm{gm\ cm^{-3}} \,, \quad h_0 = 6.4 \ \mathrm{km} \,.$$

- the horizontal depth of the atmosphere is $X \simeq 3.6 \times 10^4 \ \mathrm{gm\ cm^{-2}}$ while its vertical depth is $\simeq 1.3 \times 10^3 \ \mathrm{gm\ cm^{-2}}$ (values which adequately describe the density of the stratosphere)
- concerning the atmospheric composition, a good approximation, valid up to a height of 100 km, is 78.4% nitrogen, 21.1% oxygen and 0.5% argon. This leads to an average atomic number of $\langle A \rangle = 14.5$

for a detailed discussion of the cascade formalism see e.g. R. Gauld et al., JHEP (2016) 130, or M. Thunman, G.Ingelman, P. Gondolo, Astropart.Phys. 5 (1996) 309-332

Development of air-showers and lepton fluxes

- may be described by a set of **CASCADE EQUATIONS**

The flux $\phi_j(E_j, X)$ of a particle j with energy E_j that has traversed a slant depth X is given by:

$$\frac{\mathrm{d}\phi_j}{\mathrm{d}X} = -\frac{\phi_j}{\lambda_j} - \frac{\phi_j}{\lambda_j^{\mathrm{dec}}} + \sum_k S_{kj}(E_j, X)\,,$$

where λ_j is the interaction length (the average amount of atmosphere (in g/cm^2) traversed between successive collisions with air nuclei), λ_j^{dec} is the decay length, and S_{kj} are '(re)generation functions' describing the production of particle j from particle k. The (re)generation function is:

$$S_{kj}(E_j, X) = \int_{E_j}^{\infty} \frac{\phi_k(E_k', X)}{\lambda_k(E_k')} \frac{\mathrm{d}n(k \to j; E_k', E_j)}{\mathrm{d}E_j} \mathrm{d}E_k'\,,$$

where $\mathrm{d}n(k \to j; E_k', E_j)$ is the differential transition rate between particle species k and j (the number of particles j with energies between E_j and $E_j + dE_j$ produced in the collision of the incoming particle k with an air nucleus)

The equation says that as a particle (j) traverses the atmosphere, its flux will decrease when the particle undergoes an interaction (thus losing energy) or decays, as well as increase from the decay or interaction of other particle species (k)

Development of air-showers and lepton fluxes

Assuming that the particle flux factorises into components dependent respectively on the energy E and the slant depth X, the (re)generation function can be rewritten more simply in terms of Z-moments as

$$S_{kj}(E_j, X) = \frac{\phi_k(E_j, X)}{\lambda_k(E_j)} Z_{kj}(E_j)\,,$$

with the key property that the moment Z_{kj},

$$Z_{kj}(E_j) = \int_{E_j}^{\infty} \frac{\phi_k(E_k^{'}, X)}{\phi_k(E_j, X)} \frac{\lambda_k(E_j)}{\lambda_k(E_k^{'})} \frac{\mathrm{d}n(k \to j; E_k^{'}, E_j)}{\mathrm{d}E_j} dE_k^{'}\,,$$

is independent of the slant depth X (which cancels in the ratio of fluxes)

- **a set of coupled differential equations**:

$$\frac{\mathrm{d}\phi_{\boldsymbol{p}}}{\mathrm{d}X} = -\frac{\phi_{\boldsymbol{p}}}{\lambda_{\boldsymbol{p}}} + Z_{pp}\frac{\phi_{\boldsymbol{p}}}{\lambda_{\boldsymbol{p}}} \text{ (protons)}$$

$$\frac{\mathrm{d}\phi_{\boldsymbol{m}}}{\mathrm{d}X} = -\frac{\phi_{\boldsymbol{m}}}{\rho \mathrm{d}_{\boldsymbol{m}}(E)} - \frac{\phi_{\boldsymbol{m}}}{\lambda_{\boldsymbol{m}}} + Z_{mm}\frac{\phi_{\boldsymbol{m}}}{\lambda_{\boldsymbol{m}}} + Z_{pm}\frac{\phi_{\boldsymbol{p}}}{\lambda_{\boldsymbol{p}}} \text{ (mesons)}$$

$$\frac{\mathrm{d}\phi_{\boldsymbol{l}}}{\mathrm{d}X} = \sum_m Z_{m\to l}\frac{\phi_{\boldsymbol{m}}}{\rho d_{\boldsymbol{m}}} \text{ (leptons)}$$

Development of air-showers and lepton fluxes

The solution of these equations is in general quite involved (Monte Carlo methods needed)

- but there are simple (approximate) asymptotic analytic solutions $\Rightarrow$

The equation for the proton flux can be trivially integrated to give

$$\phi_p(E, X) = \phi_p^{(0)}(E) \exp\left(-X/\Lambda_p(E)\right) ,$$

where $\Lambda_p(E) \equiv \lambda_p(E)/(1 - Z_{pp}(E))$ is the nucleon attenuation length that depends in general on the nucleon's interaction length in the atmosphere: $\lambda_p(E) = \langle A \rangle / N_0 \sigma_{pA}(E)$, where $\langle A \rangle = 14.5$ is the average atomic number of air molecules, N_0 is Avogadro's number, and the total inelastic proton-air cross-section is denoted by σ_{pA}.

Then, the meson flux in the two asymptotic regions reads:

- at low energies the interaction and regeneration terms neglected

$$\phi_m^{\rm low}(E) = \phi_p^{(0)}(E) \frac{Z_{pm}(E)}{\Lambda_p(1 - Z_{pp})} \rho d_m e^{-X/\Lambda_p}$$

- at high energies the decay terms neglected

$$\phi_m^{\rm high}(E) = \phi_p^{(0)}(E) \frac{Z_{pm}(E)}{(1 - Z_{pp})} \frac{(e^{-X/\Lambda_m} - e^{-X/\Lambda_p})}{1 - \Lambda_p/\Lambda_m}$$

Development of air-showers and lepton fluxes

The final vertical flux of leptons expected at the detector:

$$\phi_{l,m}^{\text{low}}(E) = \phi_p^{(0)}(E)\frac{Z_{pm}(E)}{1 - Z_{pp}} Z_{ml}^{\text{low}}(E) \qquad E < \epsilon_m$$

$$\phi_{l,m}^{\text{high}}(E) = \phi_p^{(0)}(E)\frac{\epsilon_m}{E}\frac{Z_{pm}(E)}{1 - Z_{pp}}\frac{\ln(\Lambda_m/\Lambda_p)}{1 - \Lambda_p/\Lambda_m} Z_{ml}^{\text{high}}(E) \qquad E > \epsilon_m$$

where ϵ_m is a critical energy below which the probability of a meson to decay is greater than it is to interact:

$$\epsilon_m = \frac{m_m c^2 h_0}{c\tau_m \cos\theta} \simeq 3.7 - 9.5 \times 10^7 \,\text{GeV}$$

- the smaller the critical energy, the longer the decay length, hence the more energy the particle will lose by interactions in the atmosphere before it actually decays.

The final step in solving the cascade equations in the Z-moment approach is the geometrical interpolation of the low– and high–energy asymptotic solutions:

$$\phi_l(E) = \sum_m \frac{\phi_{l,m}^{\text{low}}(E) \times \phi_{l,m}^{\text{high}}(E)}{\phi_{l,m}^{\text{low}}(E) + \phi_{l,m}^{\text{high}}(E)} \,.$$

- sum over mesons contributing to the prompt flux (the leptonic decays of): D^0, $\bar{D}^0$, $D^\pm$, $D_s^\pm$ and $\Lambda_c^\pm$

Development of air-showers and lepton fluxes

The most crucial in our work is the nucleon to meson moment: Z_{pm} which depends on the charm production cross-section in pp-collisions:

- the generic Z-moment can be written as:

$$Z_{kj}(E_j) = \int_{E_j}^{\infty} \frac{\phi_k(E_k^{'}, X)}{\phi_k(E_j, X)} \frac{\lambda_k(E_j)}{\lambda_k(E_k^{'})} \frac{\mathrm{d}n(kA \to j; E_k^{'}, E_j)}{\mathrm{d}E_j} \mathrm{d}E_k^{'}$$

- Z_{pD}: the number distribution can be related to the differential charm cross-section:

$$\frac{\mathrm{d}n(pA \to D + X; E', E)}{\mathrm{d}E} = \frac{1}{\sigma_{pA}(E')} \frac{\mathrm{d}\sigma(pA \to D + X; E', E)}{\mathrm{d}E}$$

- we assume: $\sigma(pA \to D + X) \simeq \langle A \rangle \, \sigma(pp \to D + X)$

The charmed hadron Z-moments are given by:

$$Z_{pD}(E_D) = \int_{E_D}^{\infty} \frac{\phi_p(E_p^{'})}{\phi_p(E_D)} \frac{\langle A \rangle}{\sigma_{pA}(E_D)} \frac{\mathrm{d}\sigma(pp \to D + X; E_p^{'}, E_D)}{\mathrm{d}E_D} \mathrm{d}E_p^{'}$$

$$Z_{pD}(E_D) = \int_0^1 \frac{dx_F}{x_F} \frac{\phi_p(E_D/x_F)}{\phi_p(E_D)} \frac{\langle A \rangle}{\sigma_{pA}(E_D)} \frac{d\sigma_{pp\to D}(E_D/x_F)}{dx_F} \,,$$

where E is the energy of the D-meson, $x_F = E_D/E_p^{'}$ is the Feynman variable, σ_{pA} is the inelastic p-Air cross section and $d\sigma/dx_F$ is the differential cross section for the charmed meson production $\Rightarrow$ **INPUT**

Charm cross section in QCD

The basic ingredient for the prompt neutrino flux $\Rightarrow$ **pQCD charm quark production**

- the leading-order (LO) partonic processes for $Q\overline{Q}$ production $\Rightarrow$ $q\bar{q}$-annihilation and gluon-gluon fusion (dominant at high energies)

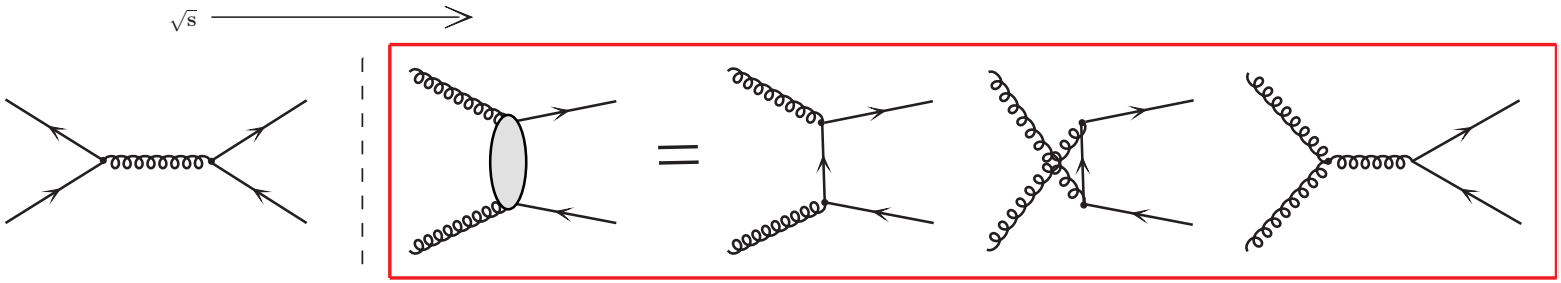

- main classes of the next-to-leading order (NLO) diagrams:

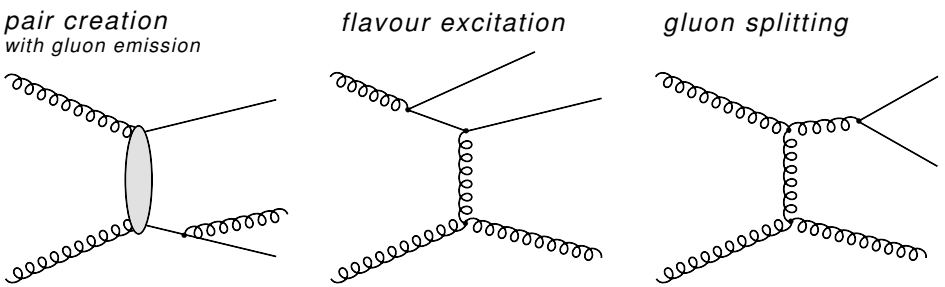

the NLO and the NNLO corrections of a special importance for charm p_T-differential cross section!

collinear approach:

- state of the art for single particle spectra at NLO (FONLL, GM-VFNS)
- MC@NLO+PS for correlations
- NNLO not available for charm/bottom

k_T-factorizaton (high-energy factorization):

- exact kinematics from the very beginning
- correlation observables directly calculable
- some contributions even beyond the NLO available (also differentially)

prompt neutrino flux $\Rightarrow$ high energy limit and far-forward charm production

k_T-factorization (high-energy factorization) approach

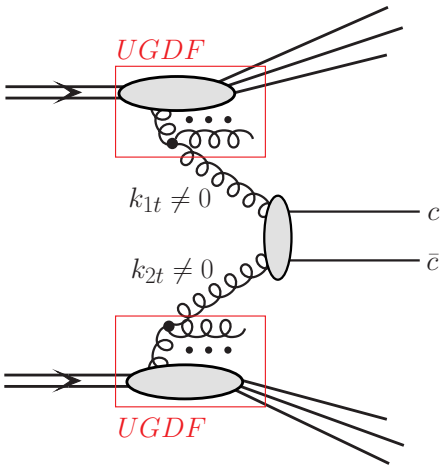

off-shell initial state partons $\Rightarrow$

initial transverse momenta explicitly included $\boldsymbol{k_{1,t}}$, $\boldsymbol{k_{2,t}} \neq \mathbf{0}$

- additional hard dynamics coming from transverse momenta of incident partons (virtualities taken into account)
- very efficient for less inclusive studies of kinematical correlations
- more exclusive observables, e.g. pair transverse momentum or azimuthal angle very sensitive to the incident transverse momenta

multi-differential cross section:

$$\frac{d\sigma}{dy_1 dy_2 d^2p_{1,t} d^2p_{2,t}} = \int \frac{d^2k_{1,t}}{\pi} \frac{d^2k_{2,t}}{\pi} \frac{1}{16\pi^2 (x_1 x_2 s)^2} \overline{|\mathcal{M}_{g^* g^* \to Q\bar{Q}}|^2}$$

$$\times \; \delta^2\left(\vec{k}_{1,t} + \vec{k}_{2,t} - \vec{p}_{1,t} - \vec{p}_{2,t}\right) \mathcal{F}_g(x_1, k_{1,t}^2, \mu)\, \mathcal{F}_g(x_2, k_{2,t}^2, \mu)$$

- the LO off-shell matrix elements $\overline{|\mathcal{M}_{g^* g^* \to Q\bar{Q}}|^2}$ available (analytic form)
- the $2 \to 3$ and $2 \to 4$ processes (higher-order) only at tree-level (KaTie Monte Carlo)
- $\mathcal{F}_g(x, k_t^2, \mu)$ - transverse momentum dependent - unintegrated PDFs (uPDFs)

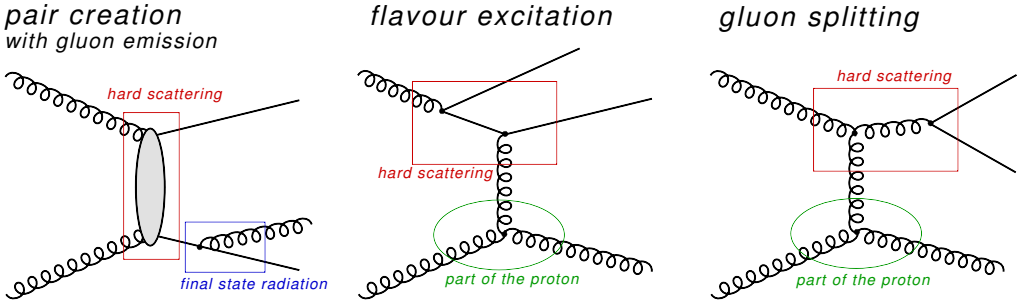

- part of higher-order (real) corrections might be effectively included in uPDF

Unintegrated parton distribution functions (uPDFs)

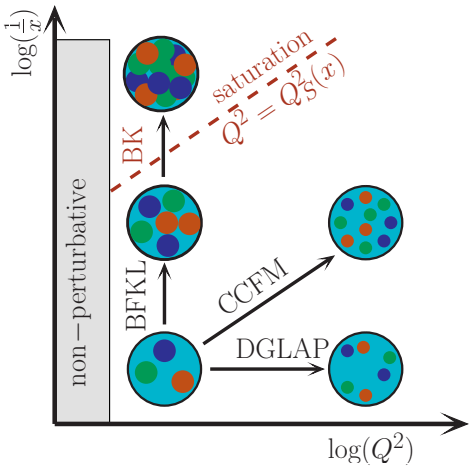

Transverse momentum dependet PDFs: $\mathcal{F}_g(x, k_t^2, \mu)$

- CCFM evolution: Jung-Hautmann (JH2013)
- Parton Branching + DGLAP: Bermudez Martinez-Connor-Jung-Lelek-Zlebcik
- linear/nonlinear BK (saturation): Kutak-Sapeta (KS)
- modified DGLAP-BFKL: Kimber-Martin-Ryskin-Watt (KMR, MRW)
- modified BFKL-DGLAP: Kwieciński-Martin-Staśto (KMS)

- hard emissions from the uPDF ⇒ higher-order corrections resummed
- k_T-fact. $g^*g^* \to c\bar{c}$ + KMR uPDF works very well for inclusive open charm and bottom mesons at th LHC (as well as for correlation observables)
- saturation effects possible to be studied within the KS uPDF
- open charm at the LHC: small-x and small/intermediate scales

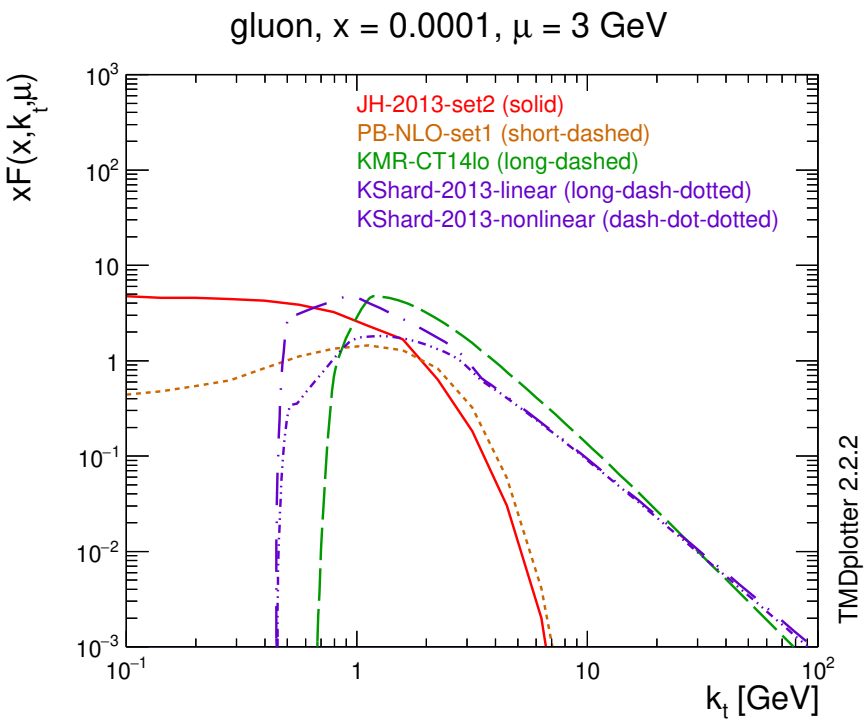

The quark to meson transition

Heavy quark to open heavy meson fragmentation: $c \to D$ and $\bar{c} \to \overline{D}$

The independent parton fragmentation picture:

- the charmed meson x_F-distributions at large x_F can be obtained from the charm quark/antiquark x_F^c-distributions as:

$$\frac{d\sigma_{pp\to D}(x_F)}{dx_F} = \int_{x_F}^{1} \frac{dz}{z} \frac{d\sigma_{pp\to charm}(x_F^c)}{dx_F^c} D_{c\to D}(z),$$

- where $x_F^c = x_F/z$ and $D_{c\to D}(z)$ is the relevant fragmentation function (FF)
- the fragmentation procedure leads to a decrease of the x_F range for meson with respect to x_F^c of the parent quark

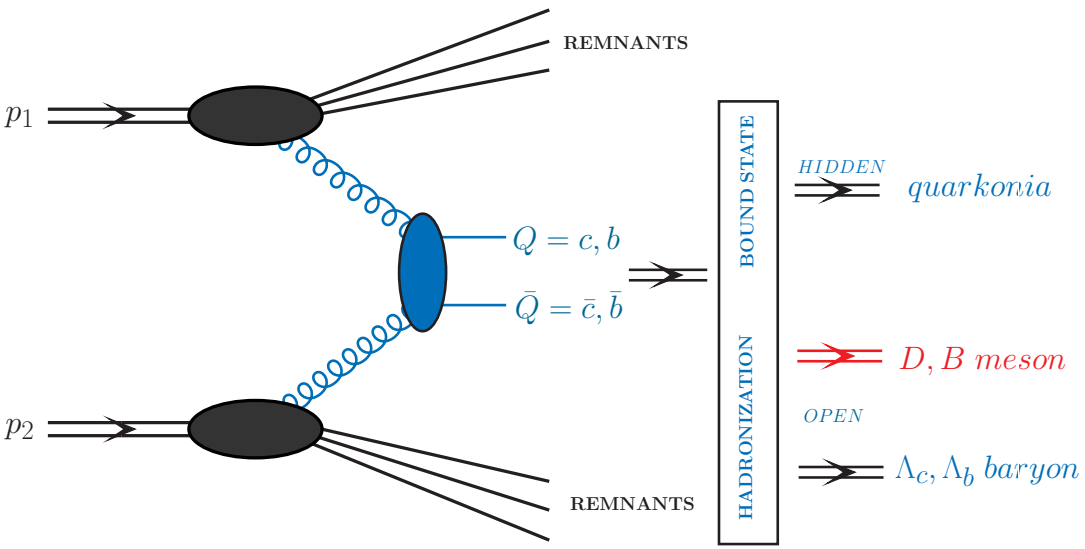

- $c \to D$: Peterson(z), $\varepsilon = 0.05$ (well known from e^+e^- data)
- $\eta_D = \eta_c$, $x_F = z \cdot x_F^c$, $z \in (0, 1)$
- fragmentation fractions well known (Particle Data Group)

Intrinsic charm at the LHC and beyond

The fixed-target data on forward open charm meson production already exists:

- Fixed-target LHCb mode at $\sqrt{s} = 86.6$ GeV (D-meson production)

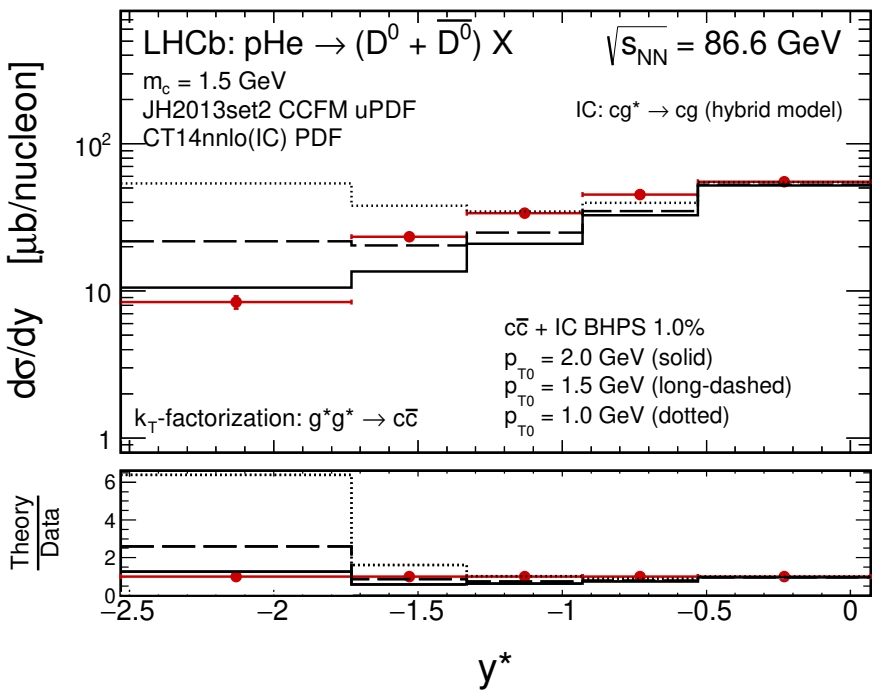

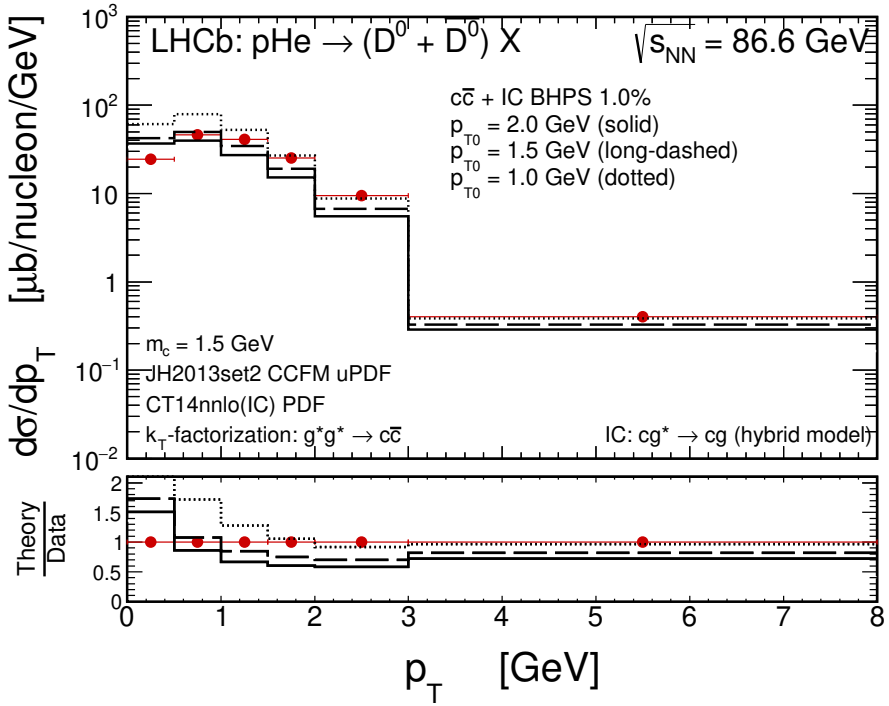

- IC BHPS 1% ⇒ the largest p_T-bin
- $p_{T0} = 2.0$ GeV ⇒ the most backward rapidity bin
- R.M, A. Szczurek, arXiv:2105.09370 [hep-ph]

Outlook

a work in progress...

The **subleading fragmentation of light quarks (u, d, s) into heavy meson (D, B)** $\Rightarrow$
a possible source of enhancement of charm production cross section at large values of x_F
(R.M, A. Szczurek, Phys.Rev.D 97 (2018) 7, 074001)

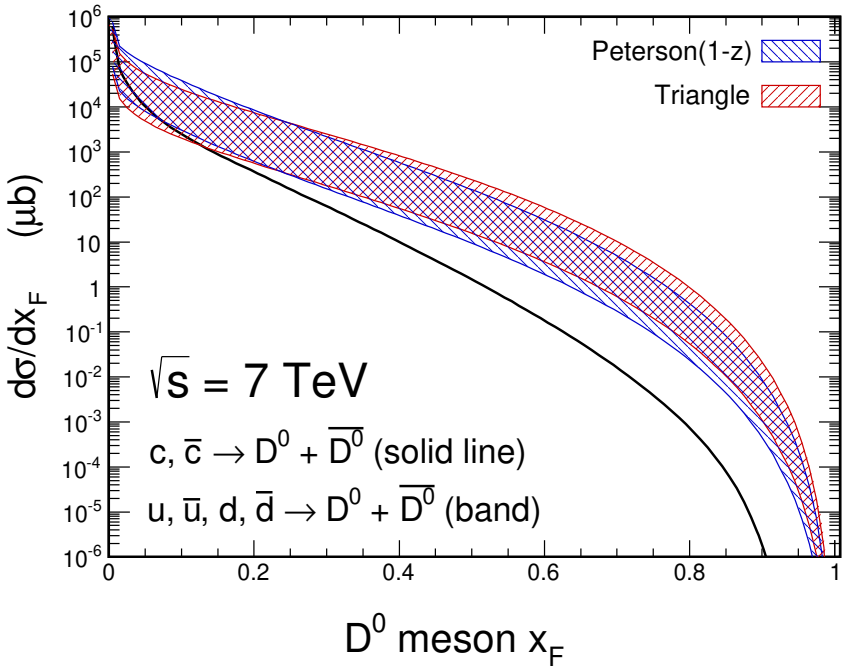

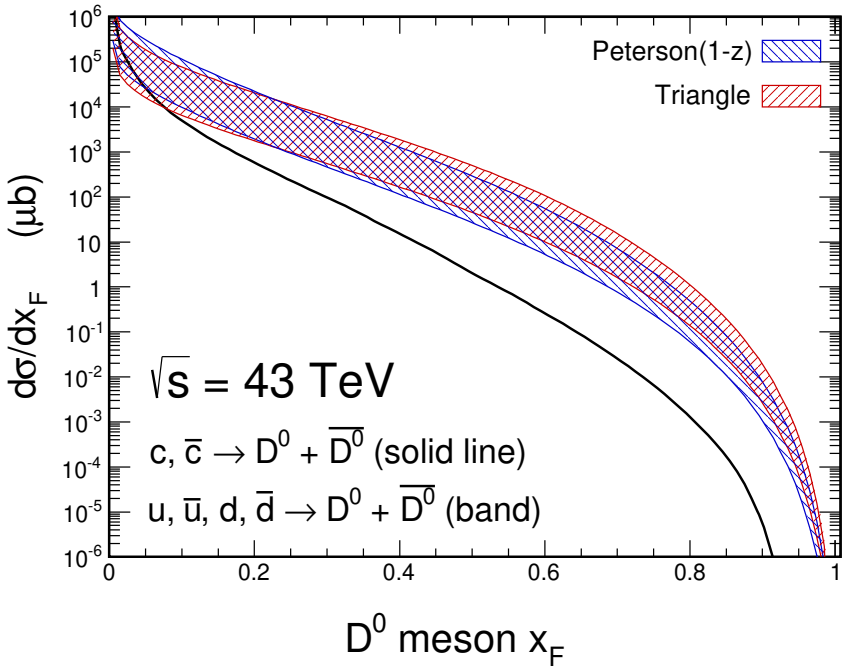

- already discussed for the ν_τ neutrino flux at IceCube
  (V.P. Goncalves, R.M, A. Szczurek, Phys.Lett.B 794 (2019) 29-35)
- might be also important for understanding the IceCube prompt ν_μ neutrino flux (stay tuned)

Prompt neutrino fluxes and saturation effects

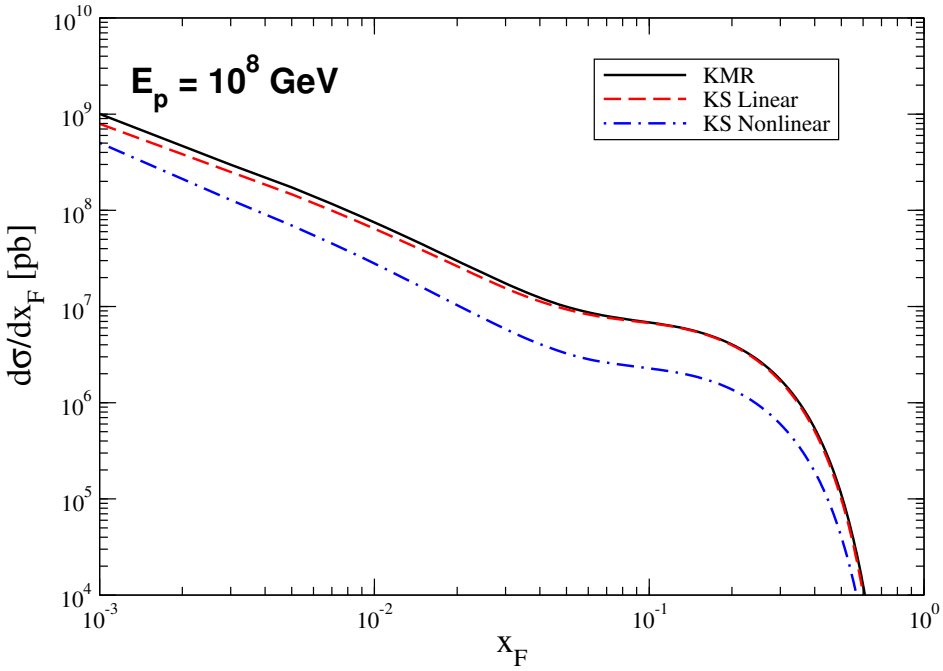

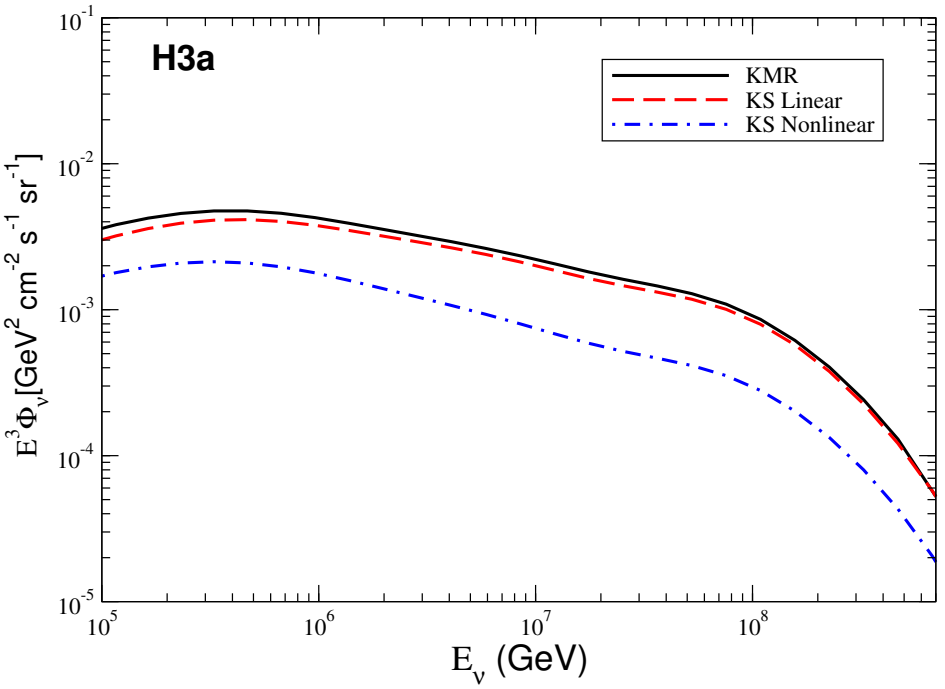

- sum of both production mechanisms: gg^*-fusion and the cg^* with IC BHPS 1%
- the KMR and KS linear predictions are similar
  $\Rightarrow$ BFKL effects not important for IceCube (which probes $0.2 < x_F < 0.5$)
- the KS nonlinear is a factor ≈ 3 smaller for $x_F = 0.2$
  $\Rightarrow$ saturation effects strongly modifies the magnitude of the distribution